January 2015

Autophagy Over The Lifespan: Using Fetal, Stem Cell, And Adult Retinal Pigment Epithelium (rpe) Cultures To Model Amd Pathogenesis

Katherine Jean Davis
Yale School of Medicine, katherine.davis@yale.edu

Autophagy Over the Lifespan:

Using Fetal, Stem Cell, and Adult RPE Cultures to Model AMD Pathogenesis

A Thesis Submitted to

Yale University School of Medicine

In Partial Fulfillment of the Requirements for the

Degree of Doctor of Medicine

By

Katherine Jean Davis

2015

Purpose: Dysfunctional autophagy in the retinal pigment epithelium (RPE) has been implicated as a therapeutic target in age-related macular degeneration (AMD). To explore how RPE autophagy changes over the lifespan and in response to phagocytosis of photoreceptor outer segments (POS), we compared stem cell-derived RPE (hESC-RPE, iPS-RPE), human fetal RPE (hfRPE), the ARPE-19 cell line, and adult RPE (ad-RPE).
Methods: RPE was cultured from 16-week human fetuses and cadaveric eyes. Stem cell-derived RPE was prepared from human embryonic stem cells (hESC-RPE) and induced pluripotent stem cells (iPS-RPE). LC3 conversion (immunoblotting) and changes in autophagy-related gene expression (qRT^2-PCR) were used to monitor autophagy. Relative maturity of RPE cultures was assessed using a panel of signature and maturation genes (qRT^2-PCR). Autophagy was manipulated with an inhibitor, Spautin-1, and inducer, Rapamycin. iPS-RPE were challenged with porcine POS daily for up to 1 month, and monitored with confocal-immunomicroscopy. The health of RPE cultures was monitored by the transepithelial electrical resistance (TER).
Results: Autophagic flux (immunoblot) increased from stem cell to a peak in 78-year-old RPE, but was reduced in 91-year-old RPE. Spautin-1 inhibited autophagy only partially—the strongest effect was on ARPE-19 and 91-year-old ad-RPE. qRT^2-PCR revealed quantitative differences in the expression of autophagy- and maturation-related genes. In iPS-RPE, the expression level of most maturation genes was most similar to hfRPE. However, iPS-RPE and ad-RPE exhibited substantially higher levels of autophagy-related genes than hfRPE. Continuous feeding of POS to iPS-RPE for three weeks lowered TER to physiologic levels. In iPS-RPE, three-weeks of exposure to POS had little effect on autophagy or signature gene-expression, but did result in the accumulation of autofluorescent granules. Continuous feeding of POS to hfRPE for one week increased the expression of autophagy genes to levels observed in iPS- and ad-RPE.
Conclusions: The characteristics of autophagy depended on the culture model: autophagy gene expression in iPS-RPE more closely resembled adult RPE than hfRPE. Partial inhibition by Spautin-1 suggests the presence of a non-canonical RPE autophagy pathway that is lost in old age. The accumulation of lipofuscin-like granules induced by POS indicates that complementary RPE cultures will be a valuable aid to explore targets for therapeutic agents for AMD.

AKNOWLEDGMENTS

First and foremost, I would not be here today without the unconditional love and support of my family, friends, and mentors, who have encouraged and motivated me for the past 27 years. To my mother and Jewels, whose selflessness inspires me on a daily basis to live a life of kindness, generosity, and compassion. To my future husband and colleague, Ryan, who keeps me smiling and sane on the toughest of days. To Dr. Lawrence Rizzolo and Dr. Ron Adelman, I am forever grateful for your dedication to my education, future, and overall wellbeing. I feel incredibly fortunate to have flourished under your mentorship, and look to you both as the epitome of an investigator, mentor, and teacher that I hope to emulate someday.

To Peter Zhao, my lab partner, colleague, and future co-resident, for your endless support, patience, and reassurance. To Dr. Shaomin Peng, Dr. Geliang Gan, and Dr. Haben Kefella, for your direction, advice, and technical expertise on this project. To Dr. Shabnam Pakneshan, for your invaluable contributions and assistance on the execution of this project's methods. To Tina Xia, who contributed to the human embryonic stem cell-derived RPE data. To Dr. Sally Temple, Dr. Tim Blenkinsop and colleagues from the Neural Stem Cell Institute (NSCI), for your generous RPE culture gifts. To Dr. John Forrest, Donna Carranzo, and Mae Geter from the Yale School of Medicine Office of Student Research, for your support of my research proposal and resulting conference presentations.

Funding: James Hirsch M.D. Endowed Yale Medical Student Research Fellowship

TABLE OF CONTENTS

Term	Abbreviation
Age-related macular degeneration	AMD
Retinal pigment epithelium	RPE
Vascular endothelial growth factor	VEGF
Pigment epithelium derived growth factor	PEDF
Photoreceptor outer segment	POS
Reactive oxygen species	ROS
Polymerase chain reaction	PCR
Mammalian target of Rapamycin	mTOR
Light chain 3	LC3
Class III phosphoinositide-3-kinase	Class III PI-3K
Beclin-1 gene	BECN1
Spautin-1	SP-1
3-methyladenine	3-MA
Human fetal RPE	hfRPE
Human embryonic stem cell-derived RPE	hESC-RPE
Induced pluripotent stem cell-derived RPE	iPS-RPE
Adult donor RPE	adRPE
Serum free medium	SFM-1
Transepithelial resistance	TER
Epithelial to mesenchymal transition	EMT
Quantitative reverse transcription polymerase chain reaction	qRT^2-PCR
Green fluorescent protein	GFP

INTRODUCTION

Age-related Macular Degeneration

Age-Related Macular Degeneration (AMD) is the leading cause of blindness in elderly populations of developed countries. In the United States alone, more than 9 million people have AMD, of whom nearly 2 million individuals have advanced AMD. Due to a rapidly aging population, the prevalence of AMD is predicted to double by 2020 [1]. AMD impairs central vision and adversely affects the ability to perform routine activities, such as reading, driving, using the phone, and recognizing faces [2]. Unfortunately, current therapies serve only to delay disease progression, not restore sight.

AMD has a complex pathology and is divided into two main forms. In the dry form (85-90% of patients), central vision loss is progressive and slow, and is associated with macular drusen formation, retinal pigment epithelium (RPE) degeneration, and photoreceptor death [3]. Significant vision loss occurs in the advanced stage of dry AMD, aptly known as "geographic atrophy" for the confluent areas of RPE and photoreceptor degeneration seen on fundus exam. Substantial vision loss is also a hallmark of the wet (exudative) form of AMD, which affects 10-15% of patients [4]. The defining feature of wet AMD is choroidal neovascularization, which presents as rapidly progressive vision loss secondary to blood vessel leakage and macular edema [4]. Since wet AMD arises in a background of dry AMD, the latter is considered a risk factor for developing exudative AMD [5].

The etiology of AMD is multifactorial, arising through a combination of genetic, environmental, and behavioral factors [6]. As its name suggests, advancing age is the greatest risk factor associated with developing AMD. Studies of identical twins suggest that genetic factors account for 46%-71% of the variation in AMD severity, with a higher

heritability estimate at more advanced stages of disease [7]. Genome-wide association studies have been instrumental in identifying genetic variants predisposing to AMD [6]. In particular, studies have confirmed association of several common variants in genes related to the alternative complement cascade, such as Y402H in the *CFH* gene on chromosome 1 [8]. In addition to genetic factors, a number of lifestyle and environmental factors have been associated with AMD, including obesity, sunlight exposure, and diet [6]. Studies consistently demonstrate a strong positive association between smoking and development of AMD, perhaps due to oxidative stress and depletion of antioxidants [9].

The multifactorial etiology and complex pathology of AMD lend to the challenging task of developing effective therapies. Although there is currently no curative treatment for AMD, the development of intravitreal anti-vascular endothelial growth factor (VEGF) therapy in the past decade has significantly improved outcomes for wet AMD, with 40% of patients gaining vision [10]. There remains no effective treatment for dry AMD, setting the stage for a major public health problem as the population ages.

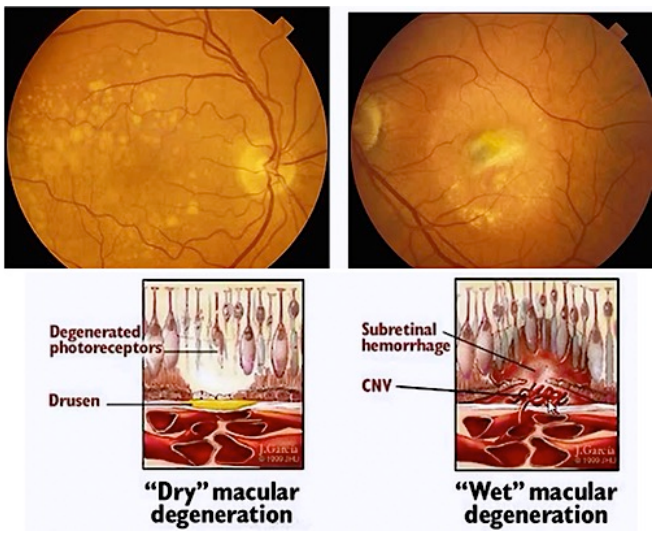

Figure 1. Age-Related Macular Degeneration (AMD) Pathogenesis. Comparing dry and wet forms of AMD. In the dry form (left), extracellular aggregates known as drusen accumulate under the retina. Drusen are seen as yellow lipid-like deposits on fundus exam. In the wet form (right), choroidal neovascularization disrupts the neural retina, leading to fluid leakage, hemorrhage, and macular edema. (Adapted from http://www.hopkinsmedicine.org/wilmer/conditions/AMDretina-detail.html).

Retinal Pigment Epithelium

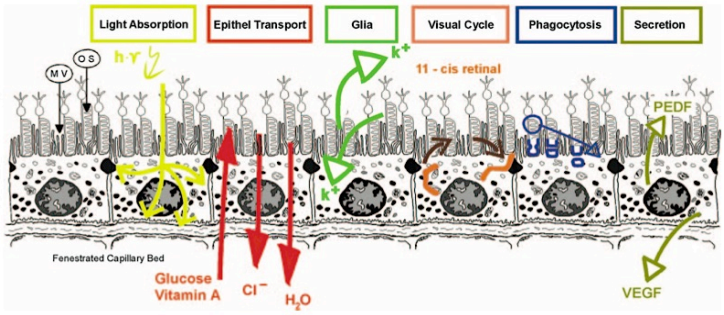

Figure 2. **Summary of Retinal Pigment Epithelium (RPE) Functions**. PEDF, pigment epithelium-derived growth factor; VEGF, vascular epithelium growth factor; Epithel, epithelium. (Adapted from: Strauss, Olaf. The Retinal Pigment Epithelium in Visual Function. Physiol Rev. 2005;85:845–881)

The RPE is a monolayer of polarized epithelial cells situated between the photoreceptor layer and Bruch's membrane, overlying the choriocapillaris. The RPE forms the outer blood-retinal barrier, and plays a vital role in neuroretinal survival. Macular RPE degeneration is a hallmark of AMD [4]. Figure 2 highlights RPE functions crucial to retinal well-being, including vitamin A metabolism and maintenance of the visual cycle, stray light absorption, and nutrient and waste exchange. Particularly relevant to this project, the RPE is responsible for phagocytosis and degradation of the distal tips (known as discs) of photoreceptor outer segments (POS) that are shed from the neural retina on a daily basis. Young and colleagues were the first group to illustrate this daily cycle of POS disc shedding, RPE disc phagocytosis, and disc renewal in the 1960s [11-13]. In the decades since, studies have identified three distinct phases of the RPE phagocytic process: 1) recognition/binding; 2) internalization; and 3) digestion [14]. Remarkably, in all vertebrate species tested, POS shedding and phagocytosis follow a diurnal rhythm [15]. Each RPE cell serves 30-40 photoreceptors, and has the highest phagocytic activity of any cell in the body [14]. Impaired RPE phagocytosis plays a role in several retinal degenerative diseases, including forms of retinitis pigmentosa [16, 17]

Given that RPE cells are post-mitotic and nonrenewable, these tasks place extraordinary metabolic demands on the RPE mitochondria and endolysosomal system over the lifetime of an individual [18]. The RPE is especially susceptible to high levels of reactive oxygen species (ROS) secondary to constant light exposure and phagocytosis of the lipid-rich POS. Over time, the resulting chronic oxidative stress and low-level inflammation contribute to RPE senescence [19, 20]. Oxidative stress leads to impaired protein degradation and the accumulation of undegraded material known as lipofuscin in lysosomes [19, 21]. Lipofuscin inhibits mitochondrial respiration and promotes protein misfolding [21]. Additionally, lipid peroxidation products have been shown to prevent lysosomal degradation of POS. Krohne et al. demonstrated that lipid peroxidation modification of POS leads to apical-to-basolateral transcytosis and extrusion of undegraded POS proteins in vitro [22]. The extruded material contributes to lipid-rich deposits known as drusen, a characteristic finding in AMD [22].

Autophagy—The Players

Unlike most other post-mitotic cells, RPE cells are not regularly replaced from resident stem cells. During its long life, the RPE relies on cellular processes to degrade and recycle senescent intracellular materials. In eukaryotic cells, autophagy is a chief intracellular method of disposing of proteins and organelles via lysosomal degradation. Unique to the autophagic pathway is the ability to recycle degraded components to use as building blocks for functional intracellular structures [23].

Autophagy is activated in situations of cellular stress, such as starvation, inflammation, and exposure to oxidative species [20, 24]. Autophagy also plays a role in cellular development, differentiation, and aging [25]. Clearance via autophagy occurs through three different methods—macroautophagy, microautophagy, and chaperone-mediate autophagy. Macroautophagy involves lysosomal degradation of cytoplasmic organelles and proteins that are delivered to the lysosome via an autophagosomal vesicle. In microautophagy, the lysosomal membrane engulfs cytoplasmic contents without the assistance of an autophagosome. Lastly, chaperone-mediate autophagy involves cellular chaperones that aid in lysosomal uptake of particular proteins [24]. Figure 3 illustrates the steps of macroautophagy, the predominant method for clearing large protein aggregates and damaged organelles: an autophagosome engulfs misfolded proteins, damaged organelles, and phagosomes, and then fuses with a lysosome. Since autophagy is a relatively conserved pathway, initial molecular and genetic studies were conducted in nonmammalian systems, namely yeast [26]. Genetic studies in yeast led to the identification of the autophagy-related (ATG) genes, of which there are nearly 30 [27].

The molecular pathways involved in autophagy are well-reviewed, and immunofluorescent and polymerase chain reaction (PCR) arrays to study autophagy are commercially available. Previous research has largely focused on the canonical autophagy pathway (Figure 3), which involves the formation of a double-membraned autophagosome around damaged organelles or protein aggregates. In the canonical pathway, autophagosomes emanate from the phagophore, which can arise from different membranes.

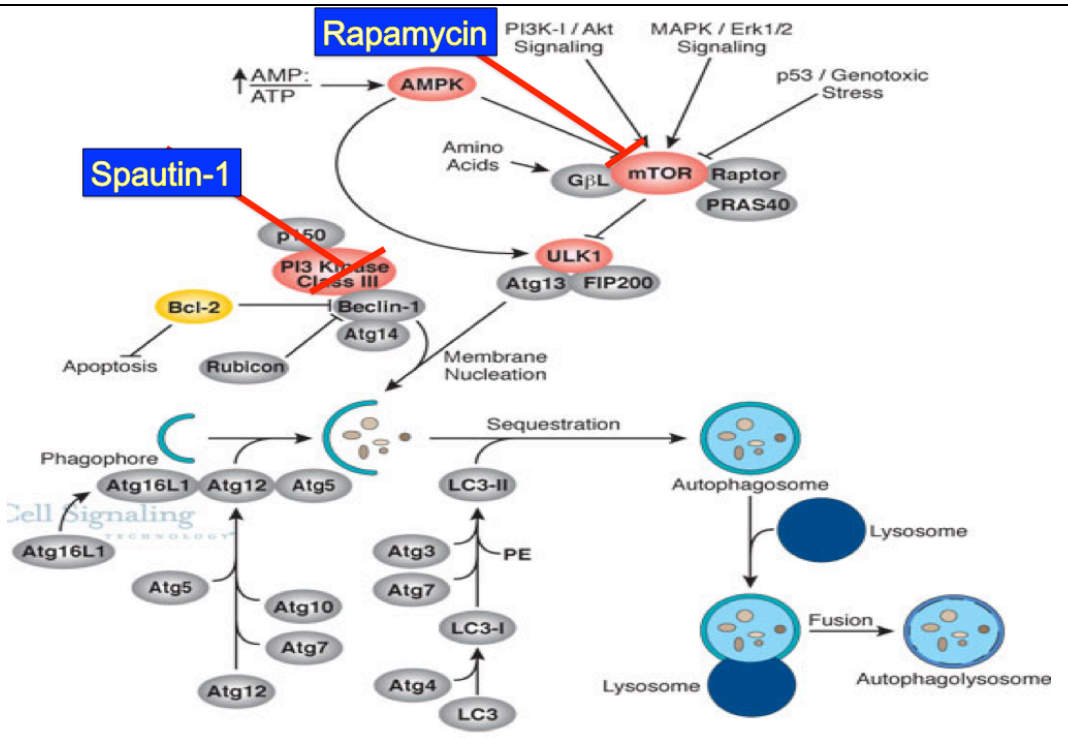

Figure 3. Canonical Autophagy Pathway. Activated mTOR (Akt and MAPK signaling) suppresses autophagy, and suppression of mTOR (Rapamycin, AMPK and p53 signaling) promotes it. Three related serine/threonine kinases, UNC-51-like kinase -1, -2, and -3 (ULK1, ULK2, UKL3) act downstream of the mTOR complex. Class III PI3K complex is required for the induction of canonical autophagy. The Atg genes control the phagophore and autophagosome formation through Atg12-Atg5 and LC3-II (Atg8-II) complexes, respectively. LC3/Atg8 is cleaved at its C terminus by Atg4 protease to generate the cytosolic LC3-I. LC3-I is conjugated to phosphatidylethanolamine (PE) in an ubiquitin-like reaction that requires Atg7 and Atg3. The lipidated form of LC3, known as LC3-II, is attached to the autophagosome membrane. (Illustration reproduced courtesy of Cell Signaling Technology, Inc. www.cellsignal.com).

Autophagy—The Modulators

Autophagosome formation is induced by Class III phosphoinositide-3-kinase (PI-3K), Beclin-1 (the mammalian ortholog of yeast Atg 6), and two ubiquitin-like conjugation systems (the Atg12-5 and Atg8 systems) [28]. The Atg12-Atg5 conjugation system promotes elongation and closure of the autophagosome, and is necessary to complete the second conjugation system, light chain 3 (LC3; Atg8 in yeast). LC3-I is a protein that is converted to its lipidated form, LC3-II, through conjugation with

phosphatidylethanolamine. LC3-I to LC3-II conversion occurs upon association with the autophagosome-lysosome fusion product [29]. This is a critical step in the completion of autophagy, as it is now recognized that an increase in autophagosome number by itself does not correlate with increased autophagic activity (also referred to as autophagic flux). Accordingly, monitoring LC3-I to LC3-II conversion is a more reliable way to assess autophagic flux, and there are commercially available LC3-II assays to do just that.

Beclin-1 plays an important role in stimulating autophagy, thus the canonical autophagy pathway is often referred to as the "Beclin-dependent" pathway. The rate-limiting PI-3K/Beclin-1 complex is also a useful target for pharmacological or small molecule inhibitors of autophagy, such as Spautin-1 (SP-1) and 3-methyladenine (3-MA) [30]. Upstream of Beclin-1 is another key autophagy modulator, the mammalian target of Rapamycin (mTOR), which negatively regulates autophagy [31]. Rapamycin (also known as sirolimus) is a natural product that inhibits the kinase activity of mTOR, and has been shown to induce autophagy *in vivo* and *in vitro* [32]. Studies have shown that Rapamycin has neuroprotective effects, making it a potential therapeutic agent for neurodegenerative disorders whose pathogenesis involves decreased or impaired autophagy, such as Alzheimer's disease and Parkinson's disease [33, 34].

In addition to the canonical, Beclin1-dependent autophagy pathway, more recent studies point to the existence of a non-canonical (i.e., Beclin1-independent) autophagy pathway. In 2007, Zhu and colleagues described stimulation of a Beclin1-independent autophagic pathway in a human neuroblastoma cell line (SH-SY5Y) by the neurotoxin 1-methyl-4-phenylpyridinium (MPP+) [35]. Beclin1-independent autophagy has been shown to play a role in differentiation [36], bacterial toxin uptake [37], and cortical

neuron death [38]. Interestingly, studies suggest that non-canonical autophagy can escape mTOR inhibition, indicating that there is also an alternative upstream regulator of autophagy [39].

In summary, genetic and molecular studies in yeast have yielded an understanding of the autophagy-related genes (and their products) involved in the mammalian canonical macroautophagy pathway. The canonical pathway is Beclin1-dependent, and can be inhibited at the PI-3K/Beclin-1 complex (e.g., with SP-1, 3-MA). Rapamycin inhibits mTOR (a negative regulator of autophagy), and is useful in stimulation of canonical autophagy. Over the past decade, evidence has grown for the existence of an alternative, non-canonical autophagy pathway that is Beclin1-independent. In contrast to canonical autophagy, non-canonical autophagosome formation does not require hierarchical intervention of all of the ATG proteins [29]. Further, non-canonical autophagy can be mTOR-independent, in which case Rapamycin would not have a significant stimulatory effect on autophagic flux.

Autophagy in AMD

If autophagy is impaired or overwhelmed, cells accumulate debris, protein aggregates, and autophagosomes [40]. Dysfunctional RPE autophagy is implicated in the pathogenesis of AMD, although the exact disease mechanisms are not clear [41, 42]. Previous work from Vittal et al. demonstrated a decline in RPE autophagic efficiency associated with both advanced age (via chronic oxidative stress) and later stages of AMD [43]. As illustrated in Figure 4, impaired autophagy in the RPE (here, due to failure of autophagosome-lysosome fusion), leads to accumulation of undegraded material,

lipofuscin formation, and eventual extrusion of autophagosomes from the basolateral side of the RPE cell to form drusen [22].

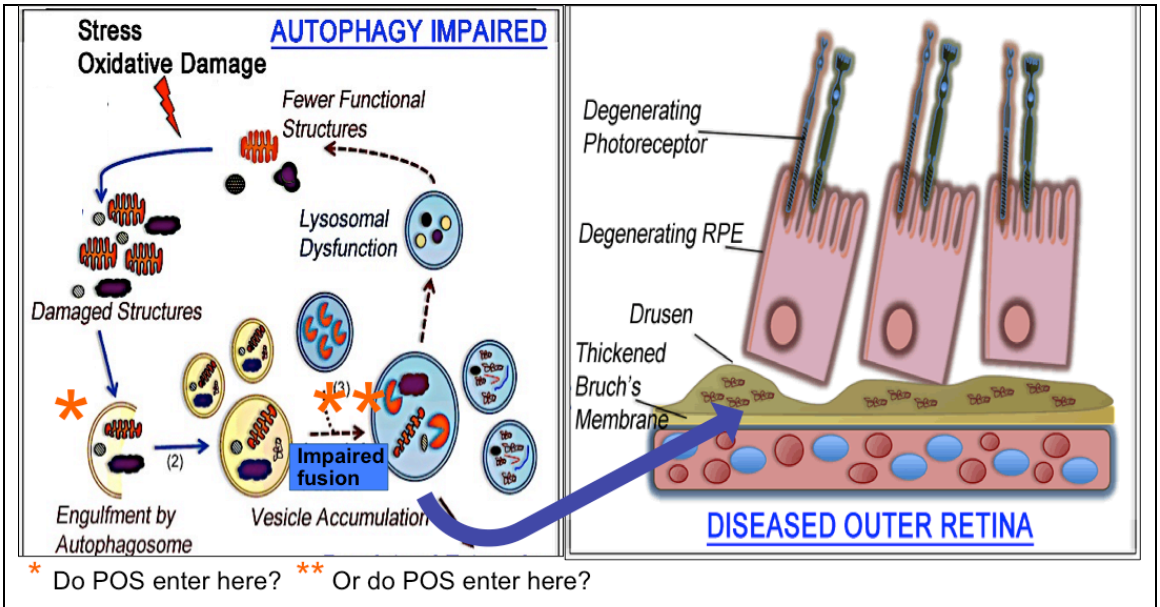

Figure 4. Impaired RPE Autophagy. Autophagy functions to dispose of proteins and organelles (e.g., mitochondria) in an intracellular process that involves autophagosome-lysosomal fusion. Age and oxidative damage contribute to damage of such structures. In the healthy cell, autophagic vesicles engulf damaged structures in phagophores to form autophagosomes, which fuse with lysosomes Phagocytosis of POS is known to interact with autophagy pathway, but the exact point of entry has not been determined. Here, two proposed points of POS entry are shown: 1) at the phagophore or 2) at the autophagosome. Within the fused autophagosome-lysosome vesicle, damaged structures are degraded and various components are recycled to rebuild functional intracellular structures. In the diseased cell (e.g., RPE in AMD), autophagy can be disrupted at multiple points (left). Impaired fusion of the autophagosome with the lysosome (step 3), lysosomal enzyme dysfunction, and phagocytic dysfunction can all result in the build-up of damaged intracellular material. This damaged material is eventually extruded from the basolateral side of the RPE, contributing to drusen formation and the thickened Bruch's membrane that are hallmarks of AMD (right).

As mentioned, besides autophagy, the RPE is responsible for phagocytosis of rod and cone outer segments (POS). RPE apical microvilli envelop the tips of rod and cone photoreceptors (Figure 4, right). The outer segment appears to be a stack of coins. These "coins" are disc membranes that are stimulated by light to initiate a signaling cascade. Each 24-hour cycle, new discs are added to the base of the segment and an equal number

are shed from the tip. As post-mitotic cells, RPE must last a person's lifetime to ensure both effective phagocytosis and lysosomal degradation of POS and recycling of visual cycle components. [14].

Although the connection between RPE phagocytosis and autophagy is well-established, the exact point where these two intracellular pathways intersect is less certain [44]. Evidence suggests that over time, aging RPE cells develop a phagocytic overload, ultimately burdening autophagic capacity and impairing normal autophagic function. Impaired ability of RPE autophagy to degrade phagocytized discs in lysosomes and recycle visual opsin components results in accumulation of lipofuscin, subretinal drusen formation, and development of AMD with central vision loss [18, 22]. Figure 4 illustrates two proposed points of entry for phagocytized POS into the autophagy pathway: 1) at the single membrane phagophore formation step, or 2) at the double membrane autophagosome formation step. Therefore, monitoring RPE phagocytosis and its downstream relation to the autophagy pathway and lysosomal degradation systems can provide insight into the pathogenesis of AMD, and identify potential therapeutic targets.

Available RPE Culture Models for Study

The best physiological model of normal, healthy RPE is derived from fetal tissues [45]. Human fetal RPE (hfRPE) represent a relatively "young" RPE phenotype, and is the preferred culture model for studying normal RPE differentiation and maturation. Fetal RPE is also useful as a model to study disease development. For instance, by manipulating hfRPE autophagy, one can study the role of autophagy-related RPE dysfunction in AMD pathogenesis. However, there are significant controversies and

challenges regarding the use of hfRPE. Firstly, there are regulatory concerns. Secondly, the availability of hfRPE is insufficient to provide adequate numbers for high throughput screening of pathogenic processes and pharmacological options. Furthermore, there is inherent variability in hfRPE, requiring an assessment of each source's functional capabilities [45]. Thus, developing alternative RPE culture model systems is both valuable and practical.

Besides hfRPE, human embryonic stem cell-derived RPE (hESC-RPE) is another *in vitro* model that represents a healthy, "immature" RPE cell. Rizzolo and colleagues demonstrated that RPE derived from pluripotent ESCs is comparable to hfRPE in regards to barrier function and gene expression [45]. The Rizzolo lab has also optimized cell culture techniques to maintain native RPE features, for instance using serum free medium (SFM-1) to achieve *in vivo*-like transepithelial resistance (TER) levels in hfRPE and hESC-RPE [46, 47]. In these conditions, hESC-RPE is functionally more mature than in differentiation medium, but still less mature than hfRPE. In addition to its utility for *in vitro* studies, hESC-RPE has a potential role in therapeutic transplantation in diseases of RPE and neural retina degeneration. In October 2014, Robert Lanza, Steven Schwartz, and colleagues reported an update on two prospective phase I/II trials of subretinal transplantation of hESC-derived RPE injected in patients with dry AMD or Stargardt's macular dystrophy [48]. Transplanted patients were followed for a median of 22 months, and results demonstrated a favorable safety profile, improvement in vision in almost half the treated patients, and increased vision-related quality-of-life [48]. However, although hESC-RPE is not associated with as many obstacles as hfRPE, widespread use is limited

by availability, and ethical and regulatory concerns. Thus, alternative RPE models are desirable in the long-term.

These concerns may be addressed by a promising new source of RPE cells, induced pluripotent stem cell-derived RPE (iPS-RPE). In 2006, a landmark paper from Kazutoshi Takahashi and Shinya Yamanaka reported the generation of 'induced' pluripotent stem (iPS) cells from mouse somatic cells by retroviral transduction of four transcription factors, Oct4, Sox2, Klf4, and c-Myc [49]. The next year, similar methods were used to generate human iPS cells from human tissues, revealing a novel way to study and treat disease using disease- and patient-specific iPS cells [50, 51]. Several groups have since demonstrated successful generation of human iPS-derived RPE from fibroblasts, T lymphocytes, and even human RPE [52-55]. Studies have shown that iPS-RPE fulfill the criteria used to evaluate stem cell-derived RPE, including 1) hexagonal cell morphology formation, 2) appearance of pigmentation, 3) apical/basal polarity, and 4) performs vital RPE functions such as phagocytosis of POS, formation of tight junctions, and secretion of growth factors [56, 57]. Additionally, concerns regarding iPS-RPE retaining memory of their former cell type are being addressed by strategies where iPS cells are derived from ocular tissues, including human RPE [55, 58]. For retinal degenerative diseases such as AMD, iPS-derived RPE has the potential to revolutionize treatment and disease outcome via graft transplantation. Furthermore, and particularly relevant to this project, iPS-RPE cells provide a new platform to study and model disease *in vitro* without the ethical and availability concerns affecting hfRPE or hESC-RPE.

For models of aged RPE, there are adult cadaveric eyes and the ARPE-19 cell line. Adult donor RPE tissue is an ideal culture model for translational research projects,

particularly those investigating degenerative diseases of the aging RPE and neural retina. Adult RPE cells from aged donor eyes have been shown to display decreased autophagic and phagocytic capacity. In one study, Schütt et al. induced aging via oxidative stress in donor RPE, and found a three-fold decrease in autophagy rates and a reduction in phagocytic capacity in these aged cells [59]. Mirroring the challenges of acquiring hfRPE, adult donor RPE is not available in adequate quantities for high throughput drug screening, although there a number of Eye Banks that have been established to help address this issue [60]. Adult RPE also has inherent differences between donor tissues, which is a possible limitation because experimental results are not necessarily generalizable. Additionally, adult RPE has proven difficult to grow in culture due to a tendency to undergo epithelial to mesenchymal transition (EMT). Recently, Blenkinsop and colleagues reported successful culture and maintenance of functional RPE monolayers by isolating intact RPE "sheets" from the adult human eye [61]. The resulting adult RPE cultures demonstrated morphological, phenotypic, and functional characteristics similar to native RPE [61]. This optimized protocol will help to standardize adult donor RPE culture, the value of which cannot be understated given the utility of adult RPE cultures for disease studies and as a cell source for transplantation therapy.

Another cell line widely used to study AMD is ARPE-19. First described by Dunn et al. in 1996, ARPE-19 is an immortalized, spontaneously-arising cell line from a 19-year-old male human donor [62]. ARPE-19 is a line with normal karyology that forms polarized epithelial monolayers on filter supports. Morphologically, ARPE-19 cells demonstrate characteristics akin to those of differentiated RPE cells, namely basolateral

infoldings, apical microvilli, and polarized distribution of cellular organelles [62]. However, with passage in culture, ARPE-19 has become increasingly sensitive to culture conditions and is losing its original phenotype, leading to difficulty replicating some characteristics of differentiation, such as pigmentation and RPE65 expression [63]. To help counter this problem, studies in Dr. Lawrence Rizzolo's laboratory and others have found low or no serum media that preserves the original phenotype [64]. Differentiated ARPE-19 phagocytizes POS more efficiently than hfRPE or iPS-RPE [65]. This observation raises the question of whether ARPE-19 is more mature than hfRPE or stem cell-derived RPE. In a comparison of *in vitro* RPE models, Ablonczy and colleagues found that properties of hfRPE more closely resembled those of a functionally normal RPE *in vivo*, whereas ARPE-19 cells resembled an aged RPE [66]. In particular, ARPE-19 hypersensitivity to VEGF, loss of pigmentation, and weaker tight junctions reflect pathologic conditions or those of an aged eye [66]. Luo et al. reported ARPE-19 cells had low TER in culture, suggesting impaired barrier function. Attempts to subclone cells from ARPE-19 were unsuccessful because the clones quickly senesced [64]. Thus, ARPE-19 may be an appropriate *in vitro* model of diseased or aged RPE, and not representative of the nondiseased 19-year-old eye from which it was isolated.

Previous Work

The discussed study was conducted under the mentorship of Lawrence Rizzolo, PhD, and Ron Adelman, MD. The Rizzolo/Adelman laboratory has demonstrated their facility with the required techniques [46]. Recently, the lab used RNA-sequencing to quantify and compare the transcriptomes of hfRPE and RPE derived from two hESC cell lines, and used electrophysiology to examine these RPE models' functionality as the

blood-retinal barrier [47]. Currently, the Rizzolo/Adelman lab is investigating whether co-culture with the retina induces the maturation of RPE. Additionally, in preliminary investigations of autophagy, the lab's mRNA microarray expression data suggested differences among the RPE cultures for the autophagy pathways. This project aimed to confirm these preliminary data with real-time quantitative reverse transcription PCR (qRT^2-PCR). Furthermore, the lab previously found that autophagy could be manipulated pharmacologically in two RPE culture models, hfRPE and ARPE19, with the use of pharmacological agents (Fig. 5-7).

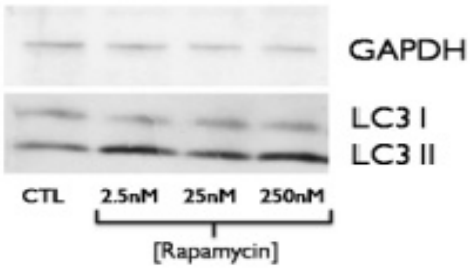

Figure 5. Autophagy Stimulation. Rapamycin (an mTOR inhibitor) increases autophagic flux in hfRPE. Association of LC3-I with autophagosomes results in its conversion to LC3-II. The increase in the ratio of LC3-II:LC3-I caused by rapamycin indicates that mTOR is a negative regulator of autophagy.

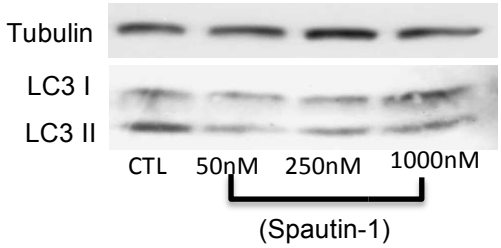

Figure 6. Autophagy Inhibition. Spautin-1 (SP-1) inhibits autophagy through its effects on Beclin-1 in ARPE-19. This is illustrated here by a decreased LC3-II:LC3-I ratio with increasing doses of Spautin-1.

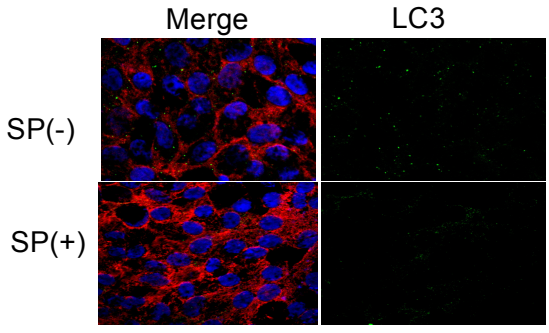

Figure 7. GFP-LC3 Immunofluorescence. SP-1 inhibits Beclin-1, and prevents the association of LC3 with autophagosomes in hfRPE. Normally, the lipidated form of LC3 (LC3-II) associates with autophagosomes, which then fuse with lysosomes. Lysosomes were inhibited with Chloroquine to prevent the degradation of LC3-II. In SP-1 treated cells, LC3 accumulation in vesicles (green puncta) is diminished, and the pool of MITF shifts from nuclei to the cytoplasm. Blue, nuclei; Red, MITF; Green, LC3.

PURPOSE AND AIMS

Dysfunctional autophagy in the RPE has been implicated as a potential therapeutic target in AMD, although the exact mechanism of disease is unclear [4, 5]. A potential contributing factor is phagocytic overload from daily RPE phagocytosis of POS, which are shed from the overlying neural retina. The post-mitotic RPE is then responsible for lysosomal degradation of POS in an autophagy-related process. Over time, autophagic capacity of the RPE is overwhelmed by this phagocytic burden, leading to accumulation of vesicles, lysosomal dysfunction, and basolateral extrusion of undegraded material from the degenerating RPE, seen clinically as drusen. We hypothesize that, since the RPE lasts the lifetime of an individual, available RPE culture models can be considered along a spectrum of phenotypic "age" in terms of autophagic function (Figure 8). From fetal life on, RPE autophagic capacity increases and plateaus as needed to compensate for acute oxidative stress and phagocytized POS. In old age, however, autophagic capacity becomes impaired and declines. On one extreme of this spectrum lie hfRPE, hESC-derived RPE, and presumably iPS-derived RPE, which represent "immature" RPE. As immature, stem cell-derived culture models, one can argue that these RPE lines may not be at the stage of development where autophagy processes have reached maturity. On the other end of the spectrum lies adult donor tissue RPE. Previous work demonstrates decreased autophagic function in this "aged" human tissue RPE. It is unclear where ARPE-19 lies along the phenotypic age continuum. Although studies have shown it to be superior in terms of POS phagocytosis, ARPE-19 has lost elements of normal RPE, and may better represent an aged or diseased RPE phenotype (Figure 8).

Characterizing phenotypic "age" of RPE cultures based on autophagic capacity can help establish a human culture model for studying AMD pathogenesis and screening pharmacological agents. I propose that there will be a difference in baseline autophagic flux and autophagy-related gene expression between available RPE culture models based on phenotypic age. Secondly, I predict that autophagic capacity can be manipulated to alter RPE culture age (for example, by feeding immature RPE cells POS, or by introducing new genes with a viral vector). Ultimately, these studies can help identify key genes or steps in the autophagic pathway as potential therapeutic targets for AMD.

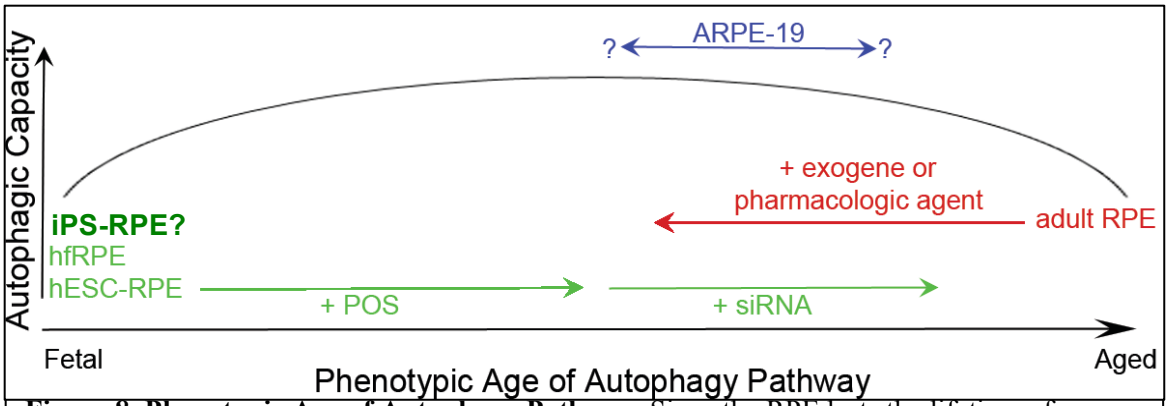

Figure 8. Phenotypic Age of Autophagy Pathway. Since the RPE lasts the lifetime of an individual, RPE cultures can be placed along a phenotypic age spectrum based on autophagic capacity. From fetal life on, RPE autophagic capacity increases and plateaus, until it is impaired in old age. We can manipulate this age spectrum to increase or decrease autophagy in various culture models (for example, by feeding immature RPE cells POS, or by introducing new genes with a viral vector). Characterizing phenotypic age of RPE cultures based on autophagic capacity can help establish a human culture model for studying AMD. (iPS-RPE: induced pluripotent stem cell-derived RPE; hfRPE: human fetal RPE; hESC-RPE: human embryonic stem cell-derived RPE)

Aim 1

Do differences in autophagy and maturation profiles of available RPE cultures help to characterize phenotypic age and explore how autophagy changes over the lifespan? For hfRPE, hESC-derived RPE, iPS-RPE, adult RPE, and ARPE-19 cell lines, relative RPE maturation can be assessed by performing real time quantitative

PCR using a panel of RPE signature and maturation-related genes [47]. Custom autophagy-specific PCR arrays allow quantification of autophagy-related gene expression. Biochemical and cellular assays help to establish baseline autophagic flux.

Aim 2

Do modulators of autophagy alter phenotypic age and autophagic flux of different RPE cultures? Having established baseline characteristics, similar assays can be used to compare RPE cultures after treatment with an autophagy inhibitor (SP-1), inducer (Rapamycin), and POS feeds.

METHODS

Cell Culture

Overview

RPE was cultured from 16-week fetuses and cadaveric human eyes (ages 48-91). Human embryonic stem cell-derived RPE was prepared from human embryonic stem cells (hESC-RPE) at the Yale Stem Cell Center. Induced pluripotent stem cell-derived RPE were prepared from induced pluripotent stem cells (iPS-RPE) of adult human RPE origin at a collaborating facility, The Neural Stem Cell Institute (NSCI; Rensselaer, NY). Adult donor RPE were also prepared at NSCI, as outlined in the group's published protocol [61]. Adult donor RPE (adRPE) and iPS-RPE were obtained or generously gifted from the NSCI. The RPE cell lines were maintained in culture media that promotes their differentiation. Prior to their use in experiments, hfRPE, hESC-RPE, and iPS-RPE were each adapted to a serum-free medium, SFM-1 [46]. ARPE-19 and adRPE were maintained in low-serum media [64]. TER, signature RPE gene expression, and cell morphology were monitored as markers for the health of RPE cultures.

Human fetal RPE (hfRPE)

The research adhered to the tenets of the Declaration of Helsinki and the guidelines of the NIH Institutional Review Board. The secondary cultures of human fetal RPE cells were prepared from 16-week fetuses, and supplied by the laboratory of Sheldon Miller (National Eye Institute, Bethesda, MD). The hfRPE cells were trypsinized in 0.25% trypsin-EDTA for 10 minutes and this trypsinization was repeated three times. The cells were then resuspended in 15% serum-containing hfRPE cell culture medium. The suspensions were centrifuged for 10 minutes at 500 rpm. The serum culture medium consisted of MEM α-modified medium (Sigma-Aldrich, St. Louis, MO), fetal bovine serum (Atlanta Biologicals, Norcross, GA), N1 supplement (1:100 mL/mL; Sigma-Aldrich), glutamine-penicillin-streptomycin (1:100 mL/mL; Sigma-Aldrich), 25 μg/mL nystatin, nonessential amino acid solution (1:100 mL/mL; Sigma-Aldrich), and hydrocortisone (20 μg/L), taurine (250 mg/L), and triiodo-thyronin (0.013 μg/L). Cells were seeded onto clear cell culture inserts at 1.3×10^5 per well (12-mm diameter inserts, 0.4-μm pores, polyester membranes; Transwell; Corning Costar, Corning, NY). The wells were coated with human extracellular matrix at 10 μg in 150 μL HBSS per well (BD Biosciences, Franklin Lakes, NJ), and cured with UV light in a hood for 2 hours prior to seeding. The medium in the apical and basolateral chambers was 0.5 mL and 1.5 mL, respectively. The cultures were maintained at 37°C in a humidified atmosphere of 95% air/5% CO2. After 24 hours, the medium was replaced, and the cells were fed three times per week. The cells reached confluence in 2 to 3 days, but the TER continued to rise over the next 6 to 8 weeks. TER was monitored using an EVOM2 resistance meter with Endohm electrodes (World Precision Instruments, Sarasota, FL). Once the cultures were stable (6 weeks), they were adapted to SFM-1 over the course of 4 weeks before

conducting studies, as previously described by the Rizzolo lab [67]. SFM-1 consisted of 70% Dulbecco's modified Eagle's medium (DMEM) containing 4.5 g/liter d-glucose, 30% F12 nutrient mixture containing l-glutamine, and 1% antibiotic-antimycotic solution, supplemented with 2% B27 (Invitrogen, Carlsbad, CA). Throughout, cultures were maintained at 37°C in a humidified atmosphere of 95% air/5% CO2.

Stem cell-derived RPE

Human embryonic stem cell-derived RPE (hESC-RPE)

Human embryonic stem cell-derived RPE was prepared by members of the Rizzolo lab from the H1 and H9 human embryonic stem cell lines (hESC-RPE) at the Yale Stem Cell Center, by the method of Idelson et al. [68]. Briefly, stem cells were cultured and passaged on Matrigel-coated dishes (BD Biosciences). Embryoid bodies were formed by treating undifferentiated stem cell colonies with 5 mg/ml dispase (StemCell Technologies, Vancouver, BC, Canada) and cultured as floating clusters in knockout serum replacement medium (KSR), composed of DMEM/F12 (1:1) medium, 14% knockout serum replacement (Invitrogen), 1% nonessential amino acids (Sigma-Aldrich, St. Louis, MO), 2 mM glutamine (Invitrogen), 50 U/ml penicillin, 50 μg/ml streptomycin (Invitrogen), and 10 mM nicotinamide (Sigma-Aldrich) in six-well ultra-low-attachment cluster plates (Costar, Corning) for 1 week. The embryoid bodies were plated on laminin-coated culture dishes (10 μg/ml) for 6 weeks. During the third and fourth weeks, KSR was supplemented with 140 ng/ml actin A (Peprotech, Rocky Hill, NJ). After the sixth week, pigmented epithelial cells were isolated by trypsinization and seeded onto laminin-coated Transwell or Snapwell culture inserts (1.3×10^5 cells per well). Differentiated cells were expanded on laminin-coated dishes and purified by weeding unpigmented cells before reseeding on culture inserts. The reseeded cultures

were maintained in KSR for 6–8 weeks, when the cultures regained their pigmentation. In some cultures the KSR was then replaced with SFM-1, which had no effect on pigmentation, and the cultures were followed for an additional 4–5 weeks.

Induced pluripotent stem cell-derived RPE (iPS-RPE)

Induced pluripotent stem cell-derived RPE were prepared from induced pluripotent stem cells (iPS-RPE) of adult human RPE origin at a collaborating facility, The Neural Stem Cell Institute (NSCI; Rensselaer, NY), and were a generous gift from Drs. Tim Blenkinsop, Sally Temple, and colleagues at the NSCI. Maintenance and RPE cell culture were conducted per their published protocol [69]. Briefly, human adult RPE cells were reprogrammed as described previously [70]. qRT-PCR was used to confirm silencing of transgenes and expression of endogenous genes, and iPS cells were then differentiated in vitro into the three germ layers [70]. Pluripotency was demonstrated by comparing gene expression of iPS cells with that of reference standards. iPS cells were then dissociated using CTK solution and passaged 1:2 onto Matrigel-coated plates (BD Biosciences, San Diego, CA, http://www.bdbiosciences.com) in TeSR medium (Stem Cell Technologies, Vancouver, Canada, http://www.stemcell.com). 70-80% of confluent cells were then transferred to KSR medium supplemented with 500 ng/ml Noggin (R&D System) and 10μM SB431542 (Tocris, Bristol, U.K., http://www.tocris.com) every day for 3 days to drive neural induction. To further drive RPE differentiation, at day 5, 1mM nicotinamide (Sigma-Aldrich, St. Louis, MO) and 150 ng/ml ACTIVIN A (R&D Systems Inc., Minneapolis, MN) were added to the KSR as well [68]. RPE colonies were identified by their characteristic "cobblestone" morphology and pigmentation (which appeared at days 25-35), and manually picked and trypsinized. Colonies were then plated at 125 x 10^3 cells per well on a 24-well Primaria plate (BD Biosciences) in RPE-taurine,

hydrocortisone, triiodothyronine (THT) medium, as described previously [71]. Cells were trypsinized again after reaching confluency, and plated at 2 x 10^6 cells per T25 Primaria flask (BD Biosciences) in RPE-THT medium and grown to form an enriched RPE monolayer. Purified RPE cells were reseeded onto Transwell filters to obtain polarized confluent electrically stable RPE monolayers in approximately 6-8 weeks [69]. Once the iPS-derived RPE were confluent, epithelial morphology was confirmed using immunostaining, and gene expression analysis demonstrated expression of RPE markers (e.g., EZRIN, DCT). Transmission electron microscopy revealed typical RPE features in these cells such as cigar-and oval-shaped melanosomes located apically, tight junctions, and apical processes. Further, the iPS cell derived-RPE monolayer cultures maintained a physiologic TER and a steady-state intracellular calcium concentration [69]. Once stable, the iPS-derived RPE were generously gifted to the mentors' laboratory on transwell filters. The cell cultures were maintained per this published protocol prior to use in studies.

ARPE-19

ARPE-19 cells were obtained from the American Type Culture Collection (passage 22; Manassas, VA). The cells were used at passage 22 and were initially maintained in tissue culture flasks for several weeks at 37^{o}C in a humidified 5% CO_2 incubator in a medium of Dulbecco's Modified Eagle Medium (Invitrogen, Carlsbad, CA) supplemented with 10% fetal bovine serum (FBS; Atlanta Biologicals, Norcross, GA), 2uM glutamine, 100 U/ml penicillin and 0.1 mg/ml streptomycin, 1x pyruvate, 25mg/ml plasmocin (InvivoGen, San Diego, CA) until they were post-confluent. Then the cells were harvested and cultured at a density of 1.8 x 10^5 in a low serum medium comprised of basal DMEM with 1% FBS, 2uM L-glutamine, 100 U/ml penicillin and 0.1 mg/ml

streptomycin, 1x pyruvate, an insulin-transferrin-selenium-BSA–linoleic acid mixture (ITS+; BD Biosciences, Bedford, MA), and 25mg/ml plasmocin on laminin-coated clear filters (Transwell; Life science). This medium yielded cultures with native morphology, as demonstrated in earlier studies from the lab [64]. The cultures rapidly became confluent. The culture media were changed bi-weekly until the culture cells were ready to use (4-5 weeks post-confluency).

Adult donor RPE

The adRPE cells were supplied by the laboratory of Dr. Sally Temple (Neural Stem Cell Institute, Rensselaer, NY) and were prepared and maintained by that laboratory protocol [61]. The group at NSCI prepared the adRPE with a primary focus on extracting RPE in "sheets" in order to preserve the junctional bonds; if done in this way, the wells grow to an epithelial monolayer after 1 month in culture [61]. Post-confluency, the Temple lab at NSCI provided the adult donor RPE cells to the Rizzolo lab on individual transwell filters that were maintained in DMEM/F12 media supplemented with high glucose, MEM Alpha (Sigma-Aldrich, St. Louis, MO), 1% Penicillin/streptomycin, N1 supplement (Sigma-Aldrich) 2% fetal bovine serum, 10mM non-essential amino acids (Sigma-Aldrich), L-glutamine 2mM, Taurine 75mg, Hydrocortisone 6μg, and Triiodo-thyronin 0.0039μg. After the adult RPE cell arrived in our laboratory, the cells were kept for a week in this "Basic Media" to stabilize before harvesting the cells for analysis.

Quantitative Reverse Transcription-Polymerase Chain Reaction

Real-time qRT^2-PCR was used to accurately quantify autophagy-related and maturation-related gene expression levels of the different RPE culture models. To capture autophagy-related and maturation-related gene expression on a larger scale, we used two

customized 96-well PCR Arrays that had primers dried in wells prior to the lab receiving them (Bio-Rad, Hercules, CA). The autophagy-specific PCR array was modeled after the Human Autophagy RT Profiler PCR Array (SA Biosciences), and originally included 86 genes involved in autophagy, including those encoding constituents of autophagosomes, lysosomes, and regulators of the autophagy pathway. The original array also included 5 "quality control" genes that ensured reliable PCR performance and RNA integrity, and 5 housekeeping genes to serve as internal controls for each reaction set. After preliminary experiments, we ordered a new set of autophagy-specific PCR arrays that included a narrowed set of genes of particular interest for the RPE culture experiments, and could fit two RPE culture cDNA samples on each plate (Figure 9, left). The maturation-specific PCR array (Figure 9, right) was custom-designed based on previous work in the lab examining signature gene expression in H1- and H9-hESC-RPE. They found that SFM-1 supports the maturation of hESC-RPE by altering gene expression of signature RPE genes towards hfRPE-like levels [47]. The signature RPE genes included on the PCR array include both the genes whose expression level changed with SFM-1 and those genes that were already expressed in hESC-RPE at hfRPE levels.

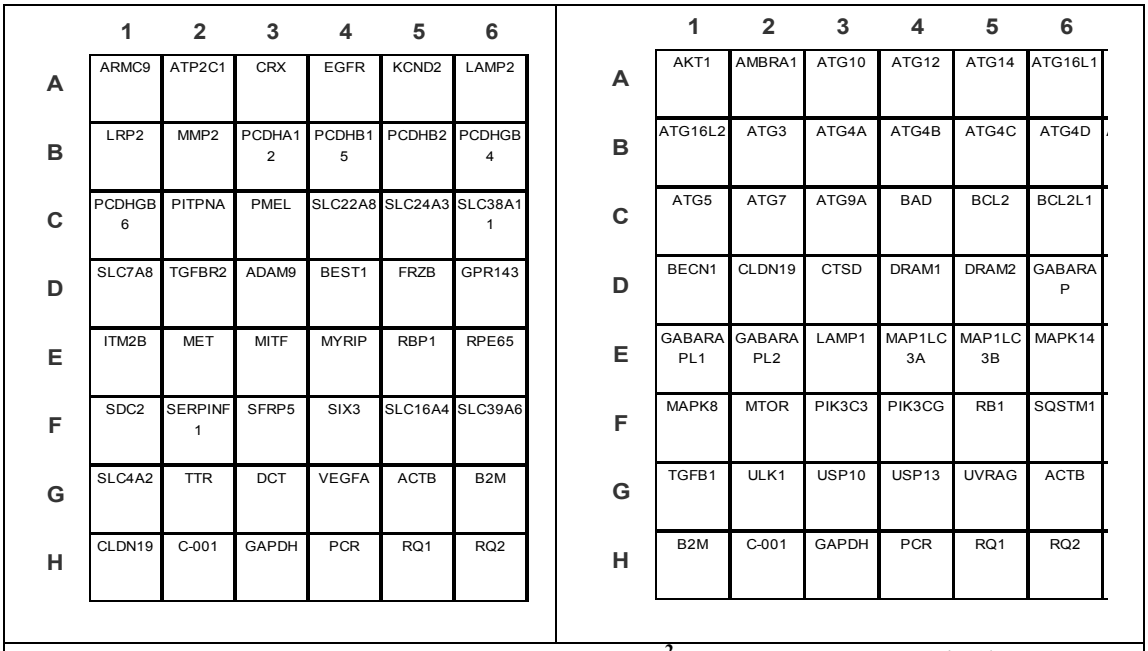

	1	2	3	4	5	6
A	ARMC9	ATP2C1	CRX	EGFR	KCND2	LAMP2
B	LRP2	MMP2	PCDHA12	PCDHB15	PCDHB2	PCDHGB4
C	PCDHGB6	PITPNA	PMEL	SLC22A8	SLC24A3	SLC38A11
D	SLC7A8	TGFBR2	ADAM9	BEST1	FRZB	GPR143
E	ITM2B	MET	MITF	MYRIP	RBP1	RPE65
F	SDC2	SERPINF1	SFRP5	SIX3	SLC16A4	SLC39A6
G	SLC4A2	TTR	DCT	VEGFA	ACTB	B2M
H	CLDN19	C-001	GAPDH	PCR	RQ1	RQ2

	1	2	3	4	5	6
A	AKT1	AMBRA1	ATG10	ATG12	ATG14	ATG16L1
B	ATG16L2	ATG3	ATG4A	ATG4B	ATG4C	ATG4D
C	ATG5	ATG7	ATG9A	BAD	BCL2	BCL2L1
D	BECN1	CLDN19	CTSD	DRAM1	DRAM2	GABARAP
E	GABARAPL1	GABARAPL2	LAMP1	MAP1LC3A	MAP1LC3B	MAPK14
F	MAPK8	MTOR	PIK3C3	PIK3CG	RB1	SQSTM1
G	TGFB1	ULK1	USP10	USP13	UVRAG	ACTB
H	B2M	C-001	GAPDH	PCR	RQ1	RQ2

Figure 9. Maturation- and Autophagy-Specific qRT^2-PCR Arrays. Customized arrays to quantify signature/maturation-related (left) and autophagy-related (right) gene expression profiles of RPE cultures. ACTB, B2M, GAPDH are housekeeping genes for internal control. PCR, RQ1, RQ2 are quality control genes. **Only one side of each PCR array is shown—the second half of each is identical, so two RPE samples can be run on each array.**

Briefly, baseline autophagy- and maturation-related gene expression of the different RPE cultures was examined using qRT^2-PCR and RNA reverse-transcribing as follows. Total RNA was isolated by following the protocol included in the RNeasy Mini Kit (Qiagen, Valencia, CA). One microgram of total RNA was reverse-transcribed to cDNA using the Quantitect Reverse Transcription Kit (Qiagen, Valencia, CA). Two RPE cultures were run on each PCR array (one on each side), and real-time qRT^2-PCR was used (iQ SYBR Green SuperMix, Bio-Rad CFX 96 thermal cycler; Bio-Rad, Hercules, CA). Experiments were performed with a minimum of two biological repeats. Relative expression of mRNA was calculated using the established $2-\Delta\Delta CT$ method [72]. Briefly, the data were first normalized relative to the expression of three housekeeping genes (GAPDH, ACTB, B2M) and then relative to the expression of a reference mRNA (e.g.,

hfRPE control cells). Error bars were calculated from independent experiments. Data is represented as the mean relative difference ± SEM of the n separate qPCR amplification reactions. Because the primers are pre-dried in the array wells, the lab is only given the amplicon context for each primer. Using the accompanying software (Bio-Rad), PCR reaction efficiency was determined for each primer, and all primers used had efficiencies >95%.

Protein Electrophoresis and Immunoblotting

Autophagic flux was determined to establish autophagic function of RPE culture models at baseline (i.e., control) and after treatment with an autophagy modulator or exposure to POS. Immunoblotting of LC3-II conversion is one method to confirm an increase in autophagy (Figure 5,6). LC3-I is converted to LC3-II upon association with autophagosomes, suggesting that an increase in the ratio of LC3-II:LC3-I is indicative of augmented autophagic flux [73]. Vice-versa, in dysfunctional autophagy, an absence of this conversion would be associated with a decreased ratio. These assays are performed in the presence of a lysosomal inhibitor to prevent the LC3-II from being degraded. Cultures were solubilized and prepared for immunoblotting, as described by the lab previously [74]. Briefly, the cultured RPE samples were washed with cold PBS and solubilized on ice in 200 μL of 25 mM Tris buffer (pH 8.0) containing 2% sodium dodecyl sulfate and 10 μL/mL protease inhibitor cocktail (Sigma-Aldrich). Melanin granules were removed by centrifugation. Detergent-resistant protein multimers were prevented from forming by adding EDTA to 5 mM along with 50 μL of 5× gel loading buffer. The samples were incubated for 10 minutes at 37°C and then for 5 minutes in a boiling water bath. Protein

concentration was determined by using the NanoDrop Lite (Thermo Scientific, Rockford, IL). Equal amounts of protein were resolved by sodium dodecyl sulfate–polyacrylamide gel electrophoresis and followed by immunoblotting. The level of β-actin staining was used as an internal standard to normalize each sample. The following primary antibodies from Cell Signaling (Danvers, MA) were used (dilutions in parentheses): rabbit polyclonal anti-LC3B (1:1000), rabbit polyclonal anti-Beclin-1 (1:1000), and rabbit monoclonal anti-PI3 Kinase class III (1:1000). Mouse monoclonal anti-rhodopsin (1:5000) was obtained from Novus Biologicals (Littleton, CO). Mouse monoclonal anti-α-tubulin (1:1,500) was obtained from Invitrogen (Grand Island, NY). The immunoblots were developed using horseradish peroxidase-conjugated secondary antibodies (1:3,000) (Thermo Scientific, Rockford, IL) and SuperSignal West Femto reagent (Thermo Scientific, Rockford, IL) and were imaged and quantified using ChemiDoc™ MP imaging system and Image Lab™ software version 4.1(Bio-Rad, Hercules, CA).

Treatment with Autophagy Modulators

Stocks of the mTOR inhibitor, Rapamycin (Cell Signaling, Danvers, MA) were prepared in dimethyl sulfoxide (DMSO) and used as an autophagy stimulator in the cell culture. If indicated, RPE cell cultures were treated with 100nM Rapamycin for two hours before the cells were harvested for immunoblotting. Spautin-1 (Cellagen Technology, Cat # C3430-2s) was also dissolved in DMSO for storage, and was used as an autophagy inhibitor at a concentration of 10μM for 24 hours. To prevent degradation of LC3, the lysosomal inhibitor Chloroquine 80ug/ml (Sigma-Aldrich, St. Louis, MO) was added to RPE cultures 2 hours before the cells were harvested.

Analysis of POS Phagocytosis by RPE Cells in Culture

Phagocytosis assays will ensure that the various RPE cell lines have ingested the presented POS. Standard phagocytosis assays involve presenting fluorescently labeled POS to monolayers of RPE cells, and then observing the POS bound to cell surfaces or internalized within the RPE cell itself. Chronic exposure to POS would result in the formation of lipofuscin if the autophagic capacity of the cells were exceeded. Porcine POS were fed cultures once every 24 hours (daily, around 8:30am) to simulate the daily pattern of disc shedding that occurs in vivo. Cultures will be monitored daily by immunofluorescence to determine the time course for the formation of lipofuscin. For ARPE-19, this process has been shown to take about 1 week [22].

Isolation of POS from Porcine Eyes

We performed POS extraction from 180 porcine eyes (obtained from the local slaughterhouse), following the published protocol from Mao and Finnemann [75]. We obtained 180 pig eyes and processed them immediately upon arrival, keeping all materials ice-cold at all times. To start, we dissected the pig eyes one by one under dim light by using a scalpel to cut into the anterior segment of the eyeball, releasing the lens and vitreous fluid. The eyeball was then flipped inside out, and a fine pair of tweezers was used to delicately dislodge the retina from the underlying tapetum. The retina was collected in a 50 mL plastic tube containing 15 mL of a Homogenization solution (for 40 mL: 20% sucrose, 20 mM Tris/Acetate pH 7.2, 2 mM $MgCl_2$, 10 mM glucose, 5 mM taurine) on ice. We continued this process until all 180 retinas were collected in three separate 50 mL tubes. Next, we shook each suspension gently for 2 minutes, and then

filtered them individually three times through a layer of sterile gauze. Under a dim light, we used a 10 mL plastic pipet to add equal volumes of the crude retina isolate to six 30 mL ultracentrifuge tubes that contained 25 mL of prepared solution of 60% sucrose, 20 mM Tris/Acetate pH 7.2, 10 mM glucose, 5 mM taurine. The tubes were then spun in an ultracentrifuge rotor at 25,000 rpm (Beckman SW-28 rotor) for 48 minutes at 4° C. The upper third of the gradient (single pink band) was collected and diluted with 5 volumes of an ice-cold wash, consisting of 20 mM Tris-Acetate pH 7.2, 5 mM taurine (per 100 mL). The diluted solution was separated into 30 mL tubes and spun for 10 minutes at 3,000 x *g*. The supernatant was removed, and the pellet was resuspended in 10 mL of a second wash (for 50 mL: 10% sucrose, 20 mM Tris-Acetate pH 7.2, 5 mM taurine). The pellets were combined and spun for 10 min at 3,000 x *g*. The supernatant was removed and the pellet was resuspended in 45 mL of a third wash (for 100 mL: 10% sucrose, 20 mM phosphate buffer pH 7.2, 5 mM taurine) and spun for 10 min at 3000 x *g*.

To prepare the POS for storage, we divided the total amount into two volumes for 1) unlabeled POS stock, and 2) FITC-labeled POS stock. The unlabeled POS stock was prepared by removing the supernatant of the halved volume, and resuspending the POS in 10 mL 2.5% sucrose in DMEM. This was diluted to 1/50 in DMEM, and then the diluted POS were counted in a cell counting chamber. The yield and concentration were calculated, and then the POS was diluted to 1 x 10^8 POS/mL with 2.5% sucrose in DMEM. The POS was stored at -80° C in aliquots of 1 mL. To prepare the FITC-labeled POS stock, the other half of the total volume was resuspended in 5 mL of the third wash (for 100 mL: 10% sucrose, 20 mM phosphate buffer pH 7.2, 5 mM taurine), and 1.5 mL of FITC stock solution was added. This was rotated at room temperature for 1 hour in the

dark. The labeled POS was then washed twice with the third wash, twice in 2.5% sucrose in DMEM, and then resuspended in 2.5% sucrose in DMEM. The labeled POS was counted and stored as described for the unlabeled POS stock.

In the original dissection, using the hemocytometer, we counted an average of 43 POS in .25 nl (i.e., one of the smallest squares). This was equivalent to 1.7×10^8 POS/mL. For each RPE cell filter, we estimated that if cells were plated at 1×10^5 cells/filter, confluency would be reached after a doubling (or possibly, tripling) of cells, making the total cells per filter equal to 2×10^5 (or 3×10^5). Generally, RPE cells are fed at 10 POS/RPE cell, so, we estimated that we would need about 12 μL of the POS solution per filter for a doubling of RPE cells, and about 20 μL of the POS solution per filter for a tripling of RPE cells. We ended up with ten 1 mL tubes of POS that were stored at -80°, and removed 1 mL tube at a time as needed for experiments. Each 1 mL tube was aliquotted into 20 400 μL eppendorf tubes (50 μL POS solution in each). Thus, each small eppendorf tube could feed about 3 RPE filters (15 μL/filter).

Fluorescence Microscopy of RPE Cultures (Control and POS-Fed)

RPE cultures were fed FITC-POS to the apical chamber for varying time periods between 3 hours and 24 hours. Additionally, RPE cultures were fed unlabeled POS to the apical chamber for varying time periods between 24 hours and 1 month (daily feedings). For feeding, RPE cells were fed 10 POS/RPE cell, which was 15 μL of POS solution (see previous section) per filter. For each feeding, the necessary number of POS-containing eppendorf tubes were thawed, and then spun down at 10,000 RPM for 2 minutes. The supernatant was removed under the cell culture hood, and the POS pellet was then washed with 1X PBS two times. The POS was then resuspended in 50 μL of DMEM and 15 μL of POS was fed to the apical side of each well.

To visualize POS, we could observe the FITC-POS in live RPE cells under a fluorescence microscope. FITC-POS could be seen on a high magnification as green dots within the RPE cells. Additionally, we could use fluorescence microscopy to visualize FITC-POS both intracellularly and attached to the RPE cell membrane. RPE cells were fed FITC-POS for varying time periods (3 hours to 24 hours) before termination of phagocytosis. Phagocytosis was terminated by washing 3 times with PBS-CM. Cells were fixed with 4% PFA in PBS-CM for 20 min, and the remaining fixative was quenched by incubating cells in 50 mM NH4Cl in PBS-CM for 20 min. Filters were washed three times with 1X PBS for 10 minutes each. Filters were then cut out of their wells and cut into halves/thirds/quarters (depending on number of conditions needed for fluorescence). Cells were then blocked with 1% BSA in 1X PBS-CM for 20 minutes. Cells were incubated with mouse monoclonal anti-rhodopsin antibody (1:1000) from Novus Biologicals (Littleton, CO), diluted in 1% BSA in PBS for 25 min. Some experiments also included incubation of cells with mouse anti-occludin (1:200) or mouse anti-ZO-1 (1:400) (Invitrogen). Filters were then washed 2 times with PBS and 1 time with 1% BSA in PBS for 5 min each. Cells were then incubated with an appropriate secondary antibody that did not conflict with FITC; for example, for rhodopsin, either Cy3 or Cy5 dyes (1:200) (Jackson Immunoresearch Laboratories, West Grove, PA). Filters were washed 2 times with PBS for 5 min each, 1 time with DAPI nuclei stain for 10 min, and 1 time with PBS for 5 min. Coverslips were mounted over filter pieces on microscopy slides with Cytoseal (Thermo-Scientific, Waltham, MA). FITC- and secondary antibody-derived fluorescence signals were imaged. Fluorescence images were acquired with an LSM 410 spinning-disc confocal microscope and processed using

AxioVision software (Carl Zeiss, Thornwood, NY). Internalized POS appeared in the FITC channel only. Surface-bound POS appeared both in the FITC channel and in the rhodopsin-specific secondary antibody image (e.g., Cy3 as red). In a color overlay of FITC (green) with secondary antibody (red), internal POS appeared green and surface-bound POS appeared yellow.

Ethical Considerations

The Mentors' lab obtains its hfRPE from the lab of Sheldon Miller at the National Eye Institute. Miller's protocols adhere to NIH Institutional Review Board guidelines, as well as the Declaration of Helsinki. One outcome of these studies may be to limit the need for tissue obtained from this controversial source.

Similarly, the use of hESC-derived RPE prompts moral concerns. The WA01 and WA09 (H1 and H9, respectively) hESC lines used in the Mentors' preliminary data and in the conducted studies are listed in the NIH hESC Registry and are approved for NIH funded research. The research was conducted under Yale ESCRO approval (project # E-09-043) for Dr. Rizzolo.

The use of adult donor RPE tissue is also associated with inherent ethical concerns. As with any donated tissue, established protocols were adhered to in order to ensure informed donor consent and proper storage and maintenance of RPE tissue. The adult donor RPE used in this project were obtained from the NSCI.

These ethical aspects were considered thoroughly in the construction and completion of this project. Experiments were conducted with the utmost of respect for established protocols of tissue acquisition. Furthermore, these studies have helped pave the way for

additional research on other potential sources of RPE as suitable culture models, including iPS-RPE and umbilical cord derived stem cell RPE.

RESULTS

Baseline Autophagic Flux Varies by RPE Culture "Age"

Autophagic flux was measured by immunoblotting LC3-I conversion to its lipidated form, LC3-II. Figure 10 demonstrates autophagic flux (LC3-II:LC3-I ratio) by RPE "age" (i.e., age of the RPE culture source) in blue. These assays are performed in the presence of a lysosomal inhibitor (Chloroquine) to prevent LC3 from being degraded, which allows measurement of amount of LC3-II (yellow), in addition to just flux. The LC3-II is normalized to β-Actin to allow comparison of relative amounts between the different RPE cultures. Although autophagic flux is the most commonly used marker of autophagic capacity, we felt it pertinent to also illustrate the relative amounts of LC3-II because there were noticeable differences in immunoblot band intensities, even after correcting for β-Actin (Figures 11,12).

Figure 10 demonstrates a gradual increase in autophagic flux from iPS-RPE and hfRPE cultures to a peak 78 year-old adult donor RPE. With the exception of 83 year-old adult RPE, autophagic flux then declined in the most aged RPE (to a low at 91 year-old RPE). LC3-II amounts were more variable, with the highest LC3-II amount seen in ARPE-19.

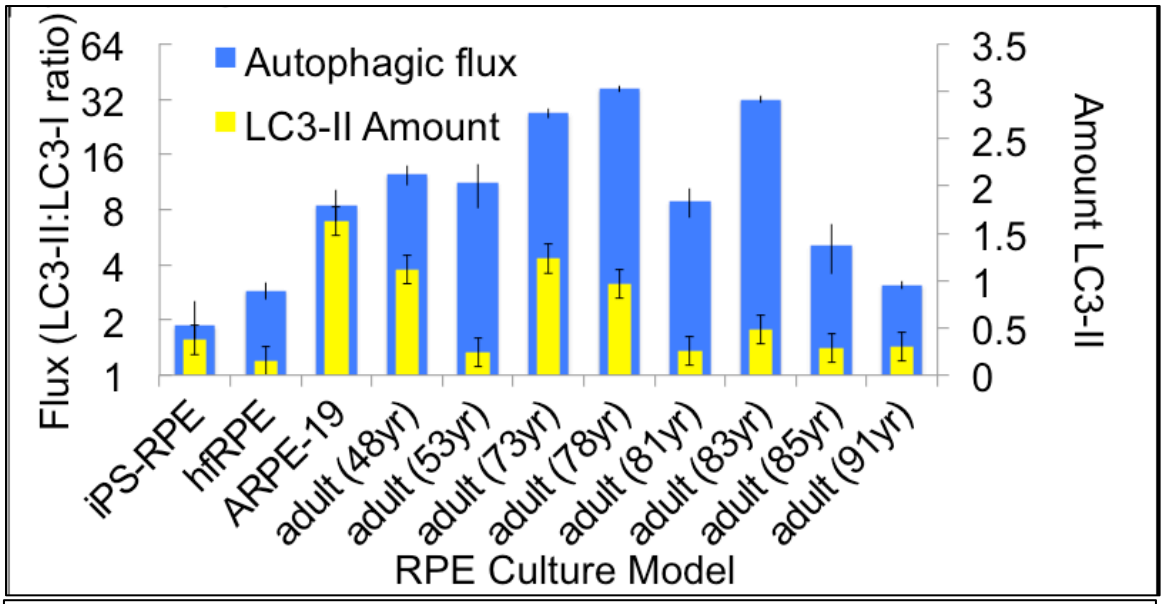

Figure 10. Autophagic Flux (LC3-II:LC3-I) and LC3-II Amount by RPE "Age." Autophagic flux increased from "immature" fetal and iPS-RPE to a peak in 78 year-old adult RPE, but declined in the most aged RPE. LC3-II was highest in ARPE-19. Error bars represent SEM for three independent experiments (n=3). LC3-II normalized to Actin.

Spautin-1 (SP-1) Partially Inhibits Autophagy in hfRPE, iPS-RPE, and Adult RPE

Figures 11 and 12 illustrate immunoblotting of RPE cultures compared at baseline and after 24-hour treatment with the autophagy inhibitor SP-1 (10μM), which targets Beclin-1 in the canonical autophagy pathway. First, there is noticeable variability in the intensity of LC3-II bands between different RPE culture models, even when accounting for relative β-Actin. Second, the ability of SP-1 to inhibit autophagic flux (LC3-I to LC3-II conversion) is not uniform across RPE cultures. 91 year-old adult RPE was the only other culture besides ARPE-19 where SP-1 strongly inhibited autophagy. Chloroquine was used to prevent degradation of LC3-II for immunoblotting. Additionally, Rapamycin (mTOR inhibitor) had little stimulatory effect on autophagy in RPE culture models, with the exception of hfRPE (not shown).

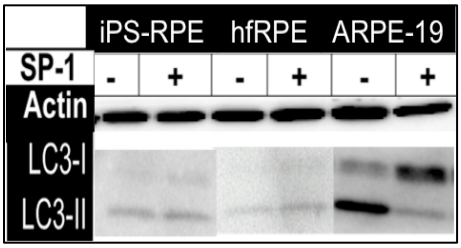

Figure 11. Spautin-1 (SP-1) Treatment. SP-1 (10μM, 24hr) only partially inhibits autophagy (LC3-I to LC3-II conversion) in iPS-RPE and hfRPE, as seen by little change between control ("-") and treatment ("+"). SP-1 strongly inhibits autophagy in ARPE-19, seen as decreased LC3-1 to LC3-II conversion with SP-1. Note the decreased intensity of the LC3-II band in iPS- and hfRPE, compared to ARPE-19.

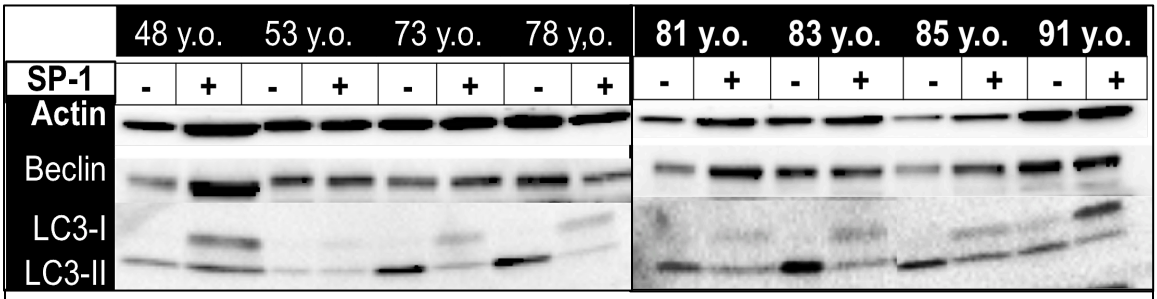

Figure 12. Spautin-1 (SP-1) Treatment of Adult RPE. SP-1 (10μM, 24 hr) only partially inhibits autophagy (LC3-I to LC3-II conversion) in almost all adult donor RPE cultures, as seen by little change between control ("-") and treatment ("+"), with the exception of 91 year-old adult RPE. Similar to its strong inhibitory effect in ARPE-19, SP-1 strongly inhibits autophagy in 91 year-old RPE, seen by decreased LC3-II:LC3-I ratio. *Note the variability in intensity of LC3-II bands.

We can dampen Spautin's inhibitory effect by feeding 91 year-old adult RPE POS. By itself, POS stimulates autophagy in 91 year-old adult RPE.

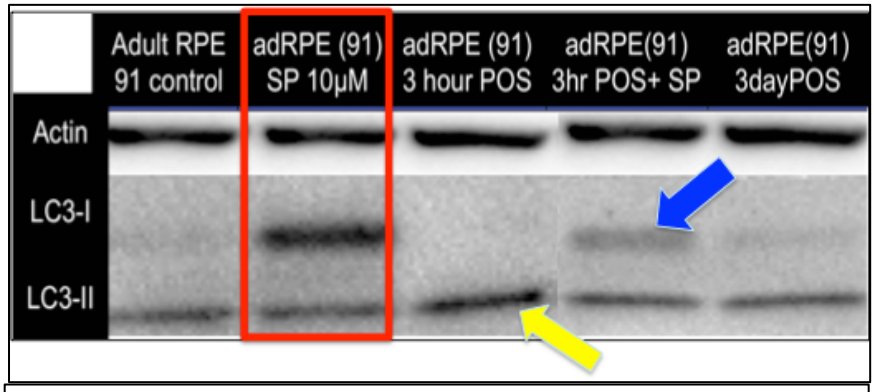

Figure 13. Effect of POS and Spautin-1 (SP-1) on 91 Year-Old Adult RPE. SP-1 treatment (10μM, 24 hr.) strongly inhibits autophagic flux (LC3-I to LC3-II conversion) in 91 year-old adult RPE (red box). POS exposure increased 91 yr. old RPE autophagic flux (yellow), and lessened the inhibitory effect of Spautin-1 (blue).

These immunoblot findings of 91 year-old adult RPE (Figure 10-12), raised the question: How will the 91 year-old RPE respond to POS feeding, given their low autophagic flux and SP-1 sensitivity? Figure 13 demonstrates 91 year-old adult RPE at

baseline (i.e., control), and after treatment with (from left to right): SP-1 (10μM), 3 hours POS only, SP-1 (10μM) *and* 3 hours of POS, and 3 days of POS only. Here, we can confirm SP-1's strong inhibitory effect on autophagic flux in 91 year-old adult RPE. However, if 91 year-old RPE were fed POS for the last 3 hours of a 24 hour SP-1 treatment, the inhibitory effect of SP-1 was dampened. Furthermore, if fed POS alone (without SP-1 treatment), 91 year-old RPE had an increased autophagic flux, .

After 3 days of POS, qRT^2-PCR of autophagy genes showed 91 year-old RPE downregulated the expression of Beclin-1 (the driver of canonical autophagy, and target of SP-1) and genes involved in the formation of a phagophore (ATG5, ATG7). ATG3, a gene involved in the formation of an autophagosome, was upregulated (Figure 14).

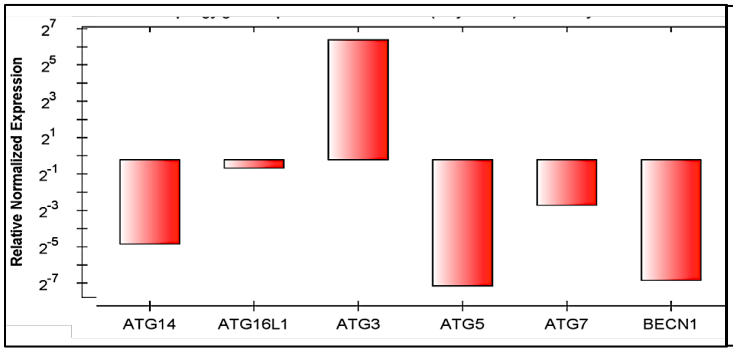

Figure 14. 91 Year-old RPE Autophagy Gene Expression After POS. After 3 days POS, qRT^2-PCR revealed 91 year-old adult RPE had downregulated gene expression of Beclin-1 and phagophore formation genes (ATG5, ATG7). The autophagosome formation gene ATG3 was upregulated. Gene expression is shown as fold-change relative to control (n=2).

Relative iPS-RPE expression of RPE signature- and maturation-related genes most resembled that of human fetal RPE.

qRT^2-PCR using a PCR array specific for maturation- and signature-related RPE genes allowed comparison of signature RPE gene expression of the various RPE culture models. Adult RPE (53 year-old and 91 year-old) demonstrated a unique maturation gene expression profile, with increased expression of a few signature genes relative to fetal RPE (not shown). One gene that was upregulated in adult RPE relative to fetal RPE was RPE65, which is involved in the visual cycle and is expressed by terminally differentiated

RPE. The gene for Transthyretin (TTR), which is apically secreted from RPE and involved in binding of retinoids, was also upregulated.

PCR array also allowed comparison of the relative expression of signature RPE genes in the hypothetical "immature" RPE cultures, specifically hESC-RPE, iPS-RPE, and hfRPE. The lab has previously demonstrated signature RPE gene expression of hESC-RPE relative to fetal RPE in a growth medium and after transition to SFM-1 medium (see Peng et al., 2013 for detailed review), and a similar maturation-related profile was seen in these repeat experiments of hESC-RPE in growth medium and SFM-1 [47]. Additionally, RPE65 was downregulated in hESC-RPE relative to hfRPE.

To characterize iPS-RPE phenotypic age, we looked at expression of maturation and signature genes relative to fetal and hESC-derived RPE. Figure 15 shows fold change in gene expression (qRT^2-PCR) of a narrowed number of pertinent signature genes in iPS-RPE relative to hfRPE. There were only two genes expressed at significantly different levels in iPS-RPE (derived from adult RPE tissue) relative to hfRPE: MMP-2 and SLC24A3 were both downregulated (starred in Figure 15). MMP2 is the gene encoding the protein matrix metalloproteinase-2, which is implicated in pathologic RPE angiogenesis and cell migration. SLC24A3 encodes for solute carrier family 24 member 3, a sodium/potassium/calcium exchanger. There was no significant difference in expression of the other 39 genes on the maturation-specific PCR array (Fig. 9, left).

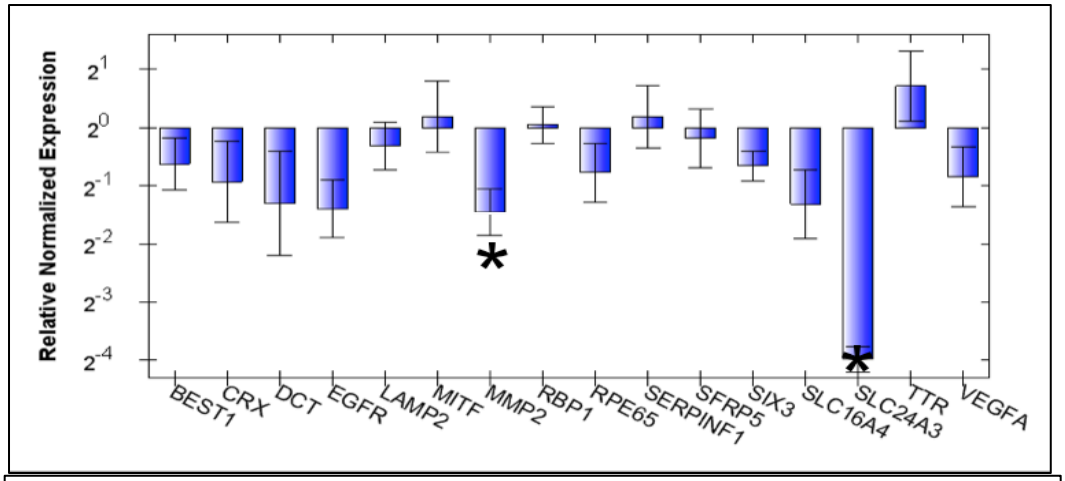

Figure 15. qRT^2-PCR of Signature Gene Expression in iPS-RPE. Expression of maturation and signature genes in iPS-RPE revealed only two genes of significant difference relative to hfRPE: MMP2 and SLC24A3 ($p<.05$). Error bars represent SEM for n=3.

Examining Baseline Autophagy-Related Gene Expression of RPE Culture Models

Having established that the maturation profile of iPS-RPE was most similar to fetal RPE, we next examined baseline autophagy-related gene expression profiles of the RPE culture models, using fetal RPE as the standard "control." Figure 16 illustrates baseline normalized autophagy-related gene expression of adult donor RPE (53 year-old) relative to hfRPE. This adult donor RPE was the same 53 year-old adult RPE that had a high autophagic flux at baseline (Figure 10). Here, we show a narrowed spectrum of genes to focus on key players in autophagosome formation, phagophore formation, and autophagy modulation (i.e., Beclin-1, mTOR). At baseline, adult RPE had general increased expression of most autophagy-related genes relative to hfRPE. Genes that were expressed at levels of significant difference ($p<.05$) are indicated and written in Figure 16. Of particular interest, 53 year-old adult RPE had significant upregulation of genes involved in autophagosome formation relative to hfRPE, including ATG3, ATG4, and

two members of the LC3 family, GABARAPL1 and MAP1LC3A. There was slight upregulation of mTOR and BECN1, around two-fold change, but this did not reach significance. ULK2, which encodes the protein Unc-51-like kinase 2, was also upregulated, near a four-fold change, but did not reach significance. ULK2 encodes a pro-autophagic protein that acts upstream of Beclin-1 and PI3 Kinase class III.

Having demonstrated an increase in expression of autophagosome formation genes in adult RPE, we next compared baseline autophagy-related gene expression of iPS-RPE relative to fetal RPE (Figure 17). Genes that were expressed at levels of significant difference ($p<.05$) are indicated in Figure 17. There was significant upregulation of autophagosome-formation genes ATG3, ATG4A, and MAP1LC3A. LAMP1, USP13 and ULK2 were upregulated, but did not reach significance. USP13 encodes for the protein ubiquitin carboxyl-terminal hydrolase 13, which is involved in tumor suppression. USP13 also reduces levels of ubiquitinated Beclin-1 when overexpressed, thus promoting autophagy.

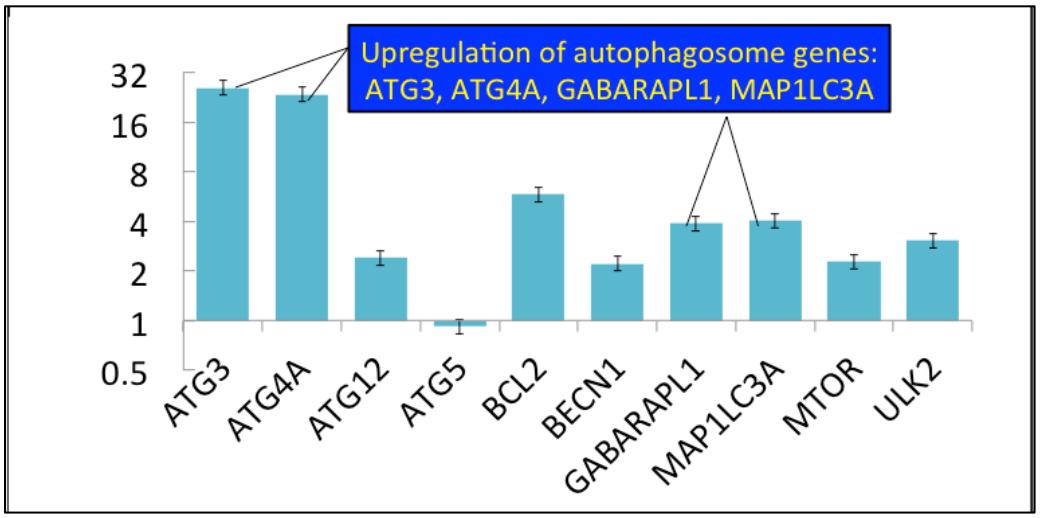

Figure 16. Baseline Autophagy-Related Gene Expression of Adult RPE. qRT^2-PCR of autophagy-related gene expression of 53 year-old Adult RPE relative to 16wk hfRPE. Error represents SEM, n=3. Genes of significant difference are written and indicated on the figure: ATG3, ATG4, GABARAPL1, MAP1LC3A ($p<.05$).

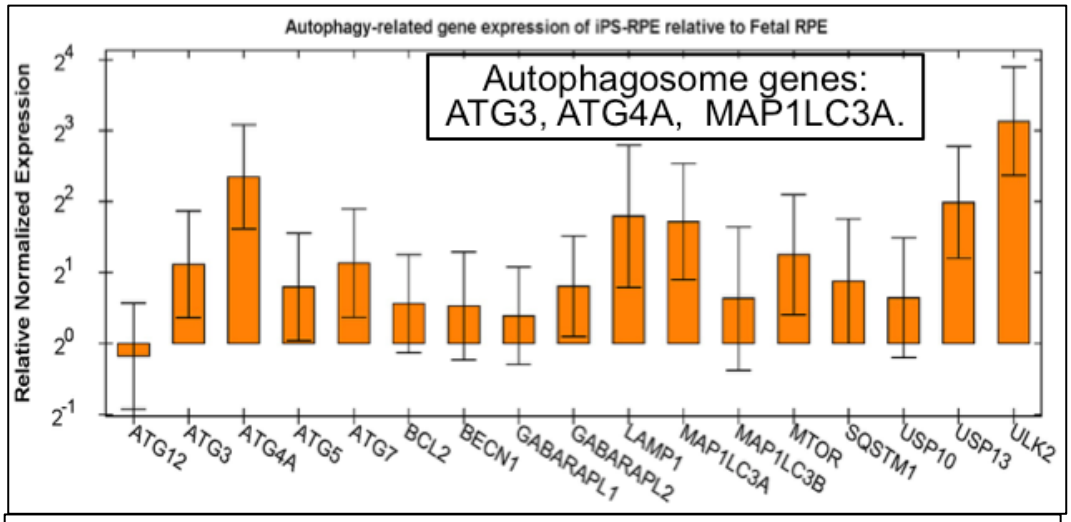

Figure 17. Baseline Autophagy-Related Gene Expression of iPS-RPE. qRT-PCR of autophagy gene expression of iPS-RPE (derived from adult human RPE tissue) relative to 16wk fetal RPE. Like adult donor RPE, iPS-RPE had increased expression of autophagosome genes. Genes of significant difference are written on the figure: ATG3, ATG4A, MAP1LC3A. ($p<.05$). Error represents SEM, n=3.

For figures illustrating fold change in gene expression (i.e., Figure 15, 16, 17, 19), it is important to note that some genes are expressed at large fold-changes that did not reach significance. This is a reflection of the fact that comparisons may look significant, but when copy number is very low, a large fold change may not reach significance.

Examining the Effect of Photoreceptor Outer Segments (POS) on RPE "Age"

The native RPE is charged with phagocytosis and lysosomal degradation of POS that are shed from the overlying neural retina on a daily basis. Phagocytic overload and subsequent autophagic dysfunction can contribute to AMD pathogenesis in the aged RPE. However, in the short-term or in relatively "immature" RPE, the effect of POS is less clear. Fetal RPE and hESC-RPE have been shown to have the ability to phagocytize POS, even though neither has seen POS at their ages (16 week and 13 week gestation,

respectively) *in vivo*. In "young" RPE that do not yet have a need for increased autophagy to handle damaged organelles and proteins, how will POS effect autophagy and phenotypic age *in vitro*?

First, to confirm phagocytic uptake of POS by hfRPE, hESC-RPE, and iPS-RPE, we fed each immature RPE FITC-labeled POS for 1 to 24 hours. Figure 18 provides a representative depiction of FITC-POS phagocytosis. Figure 18 demonstrates iPS-RPE uptake after 12 hours FITC-POS feeding, however similar uptake was observed in hfRPE and hESC-RPE. A 3-dimensional view of the RPE monolayer is shown, with FITC-labeled POS appearing as green. The nucleus appears blue (DAPI), and the secondary antibody for rhodopsin appears red (Cy3). When visualizing, pure green at the level of DAPI is FITC-POS within the RPE cell, and green+red (yellow) is POS at the RPE apical membrane, either right before or during phagocytosis.

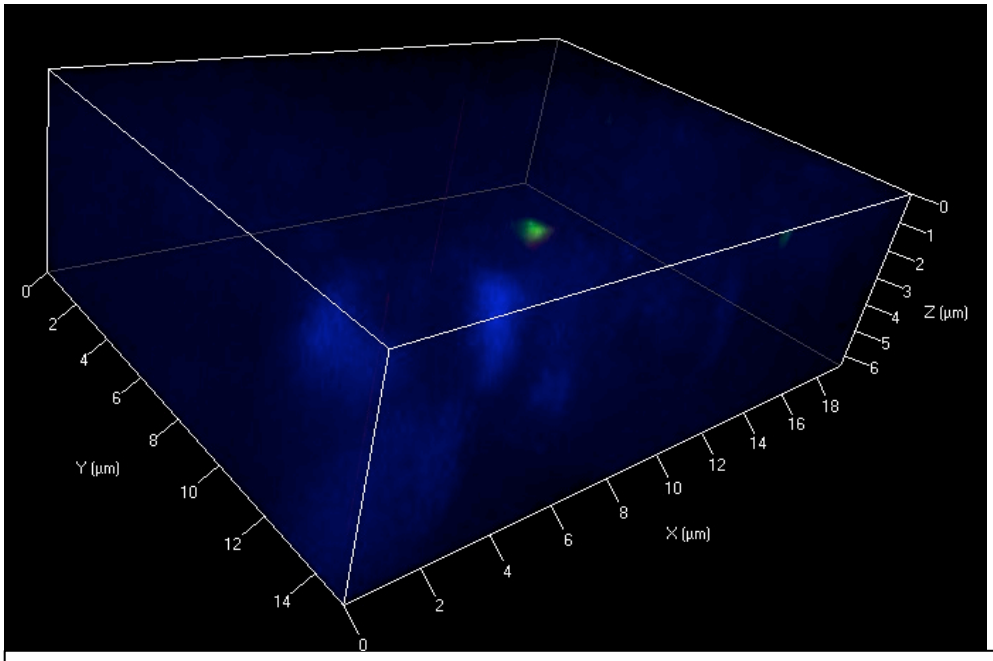

Figure 18. RPE Phagocytosis of FITC-POS. Representative phagocytosis of POS by iPS-RPE (similar uptake seen in hfRPE and hESC-RPE). Blue (DAPI) is the nucleus (i.e., intracellular), Green (FITC) is POS within the cell, Red (Cy3) is rhodopsin, Green+Red is POS at the RPE apical membrane, either during or right before phagocytosis.

To examine the effect of POS on hfRPE autophagy, we fed fetal RPE POS daily (10 POS/cell) for one week. Figure 19 illustrates the effect of 7 days POS treatment on autophagy-related gene expression in fetal RPE. Genes that were expressed at levels of significant difference ($p<.05$) are indicated in Figure 19 with a star. There was significant upregulation of the autophagosome formation genes ATG3 and LAMP1 at $p<.05$. The autophagosome gene ATG4A was upregulated at a level that trended toward, but did not reach, significance ($p<.1$). The phagophore formation genes ATG5 and ATG12 were also significantly upregulated ($p<.05$), as was the anti-apoptotic, pro-autophagic gene BCL2. The autophagosome formation-related LC3 family genes GABARAPL1, GABARAPL2, MAP1LC3A, and MAP1LC3B were upregulated, but did not reach significance.

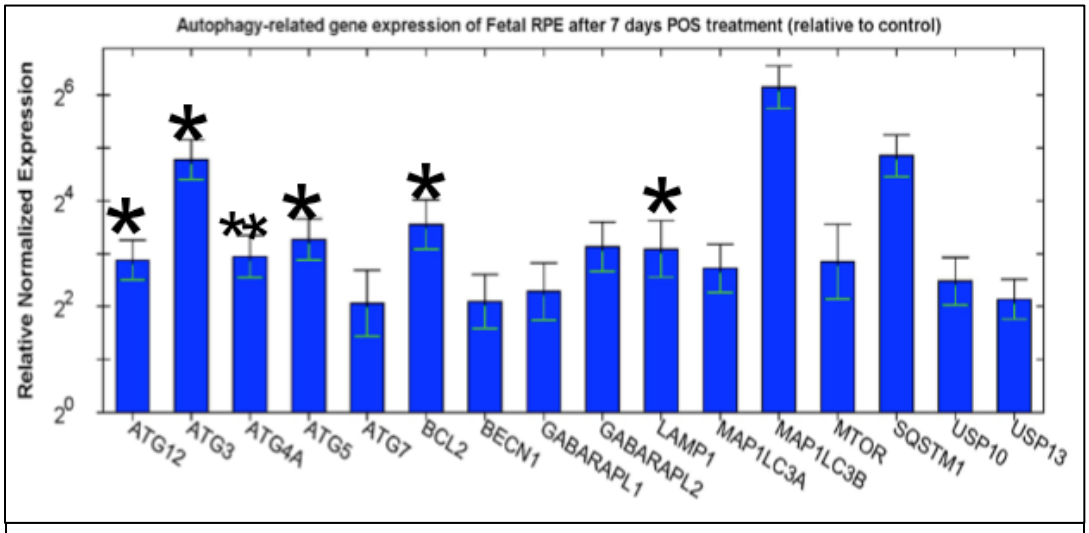

Figure 19. Autophagy-Related Gene Expression of Fetal RPE After 7 Days POS. qRT^2-PCR of autophagy gene expression of 16wk hfRPE after 1 week of daily POS feeding, relative to control hfRPE. Autophagosome genes that were upregulated in iPS-RPE and adult RPE at baseline were increased in fetal RPE after POS. (Significance*= $p<.05$) (Trend toward significance**=$p<.1$). Error bars represent SEM, n=3.

Thus, the autophagosome genes that were upregulated in iPS-RPE and adult RPE at baseline were now increased in fetal RPE after 7 days of POS exposure (Figure 18). Interestingly, in the immature hESC-RPE, although 2 days of POS resulted in a general increase in autophagy-related genes, autophagy gene expression returned to baseline by 7 days (not shown). A similar finding was present in iPS-RPE, although they started at an adult-level autophagy gene expression.

Figure 20 shows a confocal microscope image of the iPS-RPE monolayer after three weeks of daily, unlabeled POS feeding. The iPS-RPE is unstained and has an accumulation of intracellular granules. True autofluorescence is confirmed by the presence of these granules on the individual channels. This cut-view image is shown as a merge of Brightfield, Cy3, and GFP channels at 100X magnification.

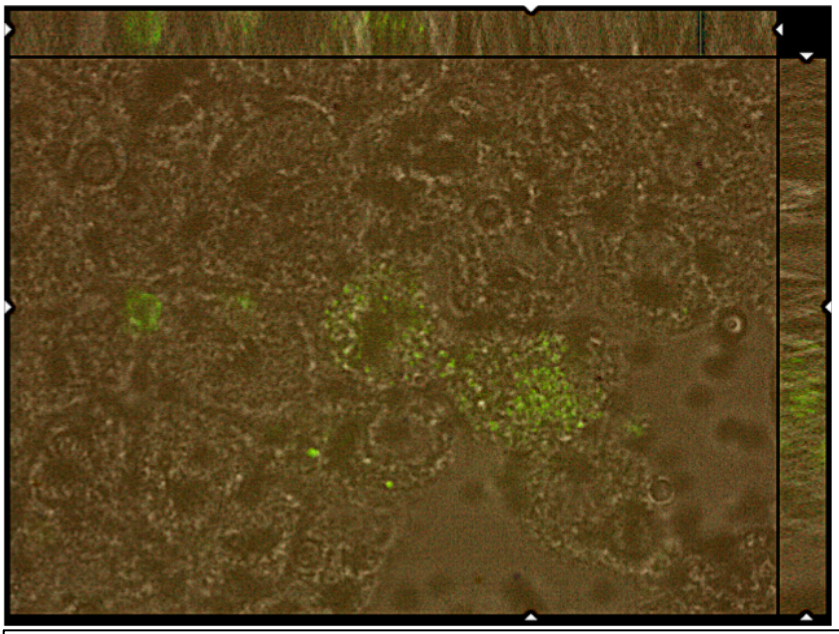

Figure 20. Accumulation of Autofluorescent Granules in iPS-RPE After 3 Weeks POS. Autofluorescent granules accumulated in iPS-RPE after 3 weeks of unlabeled POS feeds (10 POS/cell). TER was stable at physiologic levels, and iPS-RPE signature and autophagy-related gene expression was relatively unchanged from control. In this confocal image, RPE is unstained. Cut view image shows merge of Brightfield, Cy3, and GFP channels at 100X magnification. Large panel, xy plane; top ribbon, xz plane, right-side ribbon; yz plane.

DISCUSSION

Conclusions

Over 10 million people in the United States demonstrate AMD-related ocular changes, and more than 1.5 million American suffer from the advanced form of the disease. Given a globally aging population, a doubling of AMD patients is expected by 2020 [1]. Unfortunately, current therapies serve only to delay disease progression, not restore sight. AMD is particularly devastating in that it impinges on daily activities, such as reading and recognizing faces. Accumulating evidence indicates that diminished autophagic flux may contribute to the etiology of the disease. Over the lifetime of an individual and the post-mitotic RPE, phagocytic overload can burden the autophagy pathway, resulting in accumulation of vesicles, cellular debris, and lipofuscin. Undegraded material is eventually extruded from the basolateral side of the RPE as drusen, a hallmark of AMD. The precise mechanisms by which phagocytosis and autophagy interact are not clear, and one goal of this project was to better understand the connection between the two intertwined pathways. This is the first study to the author's knowledge that systematically evaluates the various RPE culture models and combines them to identify target genes and pathway points for future studies of pharmacological intervention. These studies will broaden the understanding and potential research applications of available culture models of RPE. By categorizing RPE models as phenotypically "young" or "aged" and studying them as such, one can explore the progression from healthy to diseased RPE (e.g., as occurs in AMD).

Autophagic "flux" is increasingly recognized as the preferred method to monitor autophagy, as it indicates progression from the autophagosome to the autophagosome-lysosome fusion step, which is crucial to successful completion of autophagy. Conversion of LC3-I to its lipidated form LC3-II occurs at this fusion step, so flux is often illustrated by the ratio of LC3-II:LC3-I [73]. Thus, an increase in LC3-II:LC3-I is indicative of increased autophagic flux, whereas decreased autophagic flux (i.e., decreased ratio) can occur because of impaired autophagy and in cells (e.g., "young" hfRPE) that do not yet need a high rate of autophagic degradation and recycling. As expected, we found that autophagic flux varied between the available RPE culture models. Further, we found that autophagic flux varied by RPE phenotypic "age." Specifically, autophagic capacity increased from "immature" fetal- and iPS-derived RPE, throughout middle aged adult RPE, and peaked in 78 year-old adult RPE. Flux then declined in the most aged RPE cultures, with the lowest LC3-II:LC3-I ratio for adult RPE seen in 91 year-old RPE. These findings are similar to studies of autophagy in other cell types and diseases. At 16 weeks gestation, fetal RPE have not yet been exposed to POS or experienced chronic oxidative stress, and accordingly do not need a high level of autophagy to degrade and recycle damaged organelles, misfolded proteins, or visual cycle components. However, over the lifetime of an individual, oxidative stress and daily POS phagocytosis can impair the ability of the post-mitotic RPE to perform autophagy. This is reflected in the decline in autophagic flux seen in the aged RPE cultures.

We also measured the amount of LC3-II (immunoblot) present in each RPE culture. LC3-I is converted to LC3-II upon association with an autophagosome. Studies have increasingly recognized that LC3-II alone is not sufficient to measure ongoing

autophagy. Rather than indicating successful autophagosome-lysosome fusion, increased LC3-II could instead indicate an accumulation of autophagosomes and unsuccessful completion of autophagy [60]. Interestingly, we found that LC3-II varied between different RPE cultures without any clear pattern. Of note, ARPE-19 had the highest amount of LC3-II at baseline, but not the highest flux. This suggests that there is accumulation of autophagosomes and impaired turnover of LC3-II, which may indicate dysfunctional autophagy in ARPE-19. This supports previous studies' findings that ARPE-19 is more appropriate as a model of diseased or aged RPE.

ARPE-19 was also unique in its response to the autophagy inhibitor Spautin-1, which targets Beclin-1 in the canonical autophagy pathway. Previous work by Dr. Haben Kefella (YSM 2014) confirmed near-complete inhibition of autophagic flux in ARPE-19 by 24 hour SP-1 treatment (10 μM). However, SP-1 only partially inhibited autophagy in hfRPE, iPS-RPE, and almost all adult RPE cultures. Surprisingly, 91 year-old RPE (the most aged RPE) was the only other culture where SP-1 strongly inhibited autophagy. However, we found that we could dampen SP-1's inhibitory effect by feeding 91 year-old RPE POS. Additionally, by itself, feeding POS stimulated autophagy in 91 year-old RPE, suggesting that phagocytosis of POS led to a downstream stimulation of autophagy.

In conclusion, SP-1's partial inhibition of autophagy in most RPE cultures suggests the presence of a non-canonical autophagy pathway that bypasses Beclin-1. These findings also suggest that this non-canonical pathway can be re-activated (e.g., with short-term POS feeding) in very aged (or diseased) RPE to increase autophagic capacity. However, the target for stimulation of this pathway is likely not Rapamycin, which has been proposed as a therapy for AMD in the past, given its potential as a

therapy for other neurodegenerative diseases such as Alzheimer's. We found that Rapamycin had little stimulatory effect on RPE cultures (with the exception of hfRPE), suggestive of a non-canonical autophagy pathway that is not regulated through mTOR. In fact, recently published results of phase I/II clinical trials of intravitreal and subconjunctival Rapamycin as a therapy for geographic atrophy reported that no positive anatomic or functional effects were identified, and that Rapamycin may be associated with effects that are actually detrimental to visual acuity [76, 77].

These findings inspired a return to the literature for other reports of a non-canonical autophagy pathway in RPE. As discussed, previous studies have provided evidence for a Beclin1-independent (i.e., non-canonical) autophagy pathway in cancer cell lines and infection [35-38]. In July 2013, Kim et al. reported a non-canonical form of autophagy in RPE (referred to as LC3-associated phagocytosis) that is involved in visual component regeneration through POS phagocytosis [78]. In RPE-J cells, they noted association of LC3 with single membrane phagosomes that contained phagocytized POS. This form of non-canonical autophagy was different than that previously reported and the author's findings, in the sense that it *was* Beclin1-dependent. Regardless, it provides additional support for the existence of alternative autophagy pathways in LC3, and illustrates a direct connection between the phagocytic and autophagic pathways. In contrast to Kim et al.'s finding that non-canonical autophagy depended on Beclin-1 and gene products involved in phagophore formation (specifically, Atg5), our results suggest the presence of a non-canonical, Beclin1-independent pathway that is unaffected by SP-1.

Analysis of baseline autophagy-related gene expression suggests that adult RPE cultures with high baseline autophagic flux had increased expression of key

autophagosome-forming genes (i.e., ATG3, ATG4A, GABARAPL1, and MAP1LC3), and downregulated or unchanged levels of phagophore-related genes (such as ATG5, ATG7, BECN1). These same autophagosome genes were upregulated in 91 year-old adult RPE and hfRPE after 3 days and 1 week of POS, respectively. Thus, phagocytized POS appear to merge with the autophagy pathway *after* the Beclin1-dependent phagophore formation step. Additionally, this demonstrates that autophagic function of "immature" fetal RPE and "aged" or diseased adult RPE can be pushed toward a healthy adult-like state by exposure to POS.

Figure 21 is a revised illustration of the canonical and non-canonical autophagy pathway, based on the results of this project. Canonical autophagy is shown as a Beclin1-dependent pathway, stimulated by Rapamycin and inhibited by SP-1. Here, we demonstrate the entry of phagocytized POS into the non-canonical autophagy, specifically at the point of the autophagosome. Our results suggest that genes involved in autophagosome formation are key to autophagic capacity, particularly in the aging RPE or when exposed to POS. Phagophore genes were largely unchanged or downregulated.

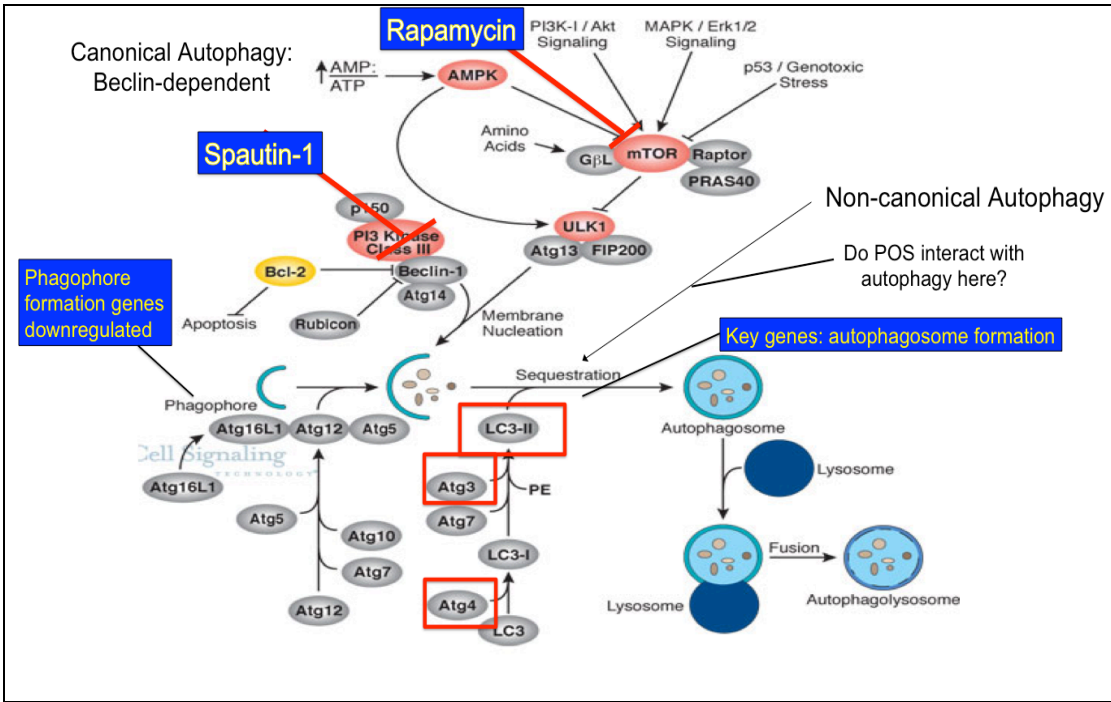

Figure 21. Canonical and Non-canonical Autophagy Pathways Revised. Canonical autophagy is Beclin1-dependent, inhibited by Spautin-1, and stimulated by Rapamycin. Autophagosome formation genes are key to a non-canonical autophagy pathway, and are upregulated after POS phagocytosis, suggesting an alternative entry point for POS. (Illustration reproduced and modified with permission of Cell Signaling Technology, Inc. www.cellsignal.com).

A secondary aim throughout this project was to characterize the maturation-related and autophagy-related gene expression profiles of iPS-RPE cell cultures. As stem cell-derived cells, iPS-RPE have been considered "immature," and are expected to lie on the "young" end of the phenotypic age spectrum in Figure 9. The iPS-RPE used in these experiments were derived from adult human RPE tissue, thus their gene expression profiles are not as well characterized as iPS-RPE derived from adult fibroblasts, which constitute the majority of previous studies on iPS-RPE [50, 57, 69, 79, 80]. PCR array of signature genes revealed that the maturation expression profile of iPS-RPE most resembled that of fetal RPE, supporting its relative immaturity. Considering this, it was surprising to find that iPS-RPE express autophagy-related genes (in particular,

autophagosome-formation genes) at adult RPE levels (Figure 17). This raises the question: do iPS derived from human adult RPE retain epigenetic markers? Future studies will help to address this issue. Interestingly, after three weeks of unlabeled POS feeding, accumulation of autofluorescent granules was observed in iPS-RPE. Transepithelial resistance (TER) remained stable at physiologic levels, and iPS-RPE signature and autophagy-related gene expression were relatively unchanged from control. Of note, previous studies demonstrate an accumulation of autofluorescent material in ARPE-19 after just 1 week of POS feeding [22]. I propose that iPS-RPE derived from adult RPE tissue have great potential as a novel source of cells for RPE transplantation therapy due to their relatively "young" phenotypic age combined with adult-like autophagic capabilities and prolonged stability in the presence of lipofuscin.

Figure 22 offers a revised hypothesis of phenotypic age among RPE cultures based on this project's results, which suggest that the most "immature" RPE culture is hESC-RPE. Unlike fetal RPE, POS feeding had no effect on the autophagy or maturation expression profiles of hESC-RPE, indicating that this RPE culture model has not developed the signaling pathways to connect phagocytosis and autophagy. Thus, hESC-RPE may not be an appropriate culture model to study AMD pathogenesis because its autophagy pathway cannot be manipulated to induce phenotypic aging. In contrast, RPE derived from 16-week human fetuses *did* have the necessary signaling pathways in place, resulting in maturation toward an adult-like autophagic state after POS exposure. This suggests that hfRPE are primed for POS exposure, which first occurs in utero at 19-20 weeks gestation. Based on signature gene expression, iPS-RPE is relatively "immature," similar to fetal RPE. However, at baseline, iPS-RPE that are derived from adult RPE

tissue have increased autophagy-related gene expression, similar to the autophagy expression profile of an adult. Specifically, genes involved in autophagosome formation are upregulated in iPS-RPE and 53 year-old adult RPE. With long term POS, iPS-RPE autophagy gene expression is relatively unchanged, though it is already at adult levels.

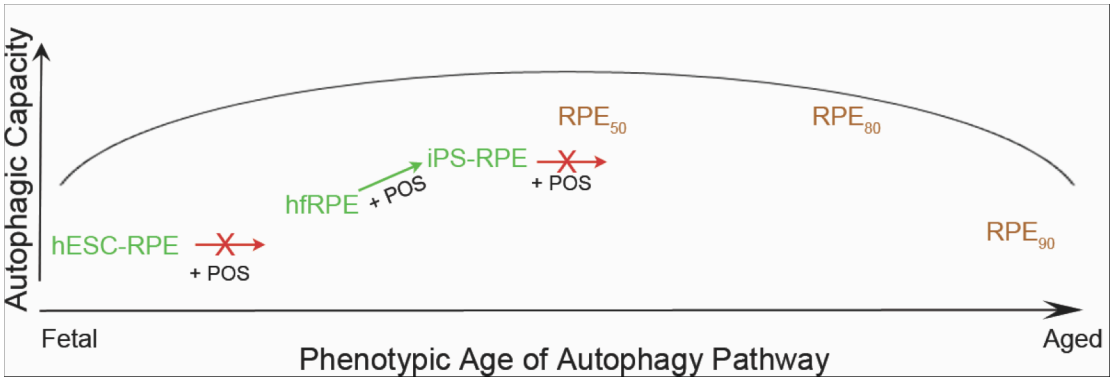

Figure 22. Phenotypic Age of Autophagy Pathway Revised. Since the RPE lasts the lifetime of an individual, RPE cultures can be placed along a phenotypic age spectrum based on autophagic capacity. From fetal life on, RPE autophagic capacity increased to peak levels in adult RPE, and was impaired in the most aged RPE. We could manipulate this age spectrum to increase autophagy in various culture models (e.g., by feeding hfRPE POS). ARPE-19 did not fit appropriately at any point on the phenotypic age spectrum, and is not included.

Adult RPE demonstrated a peak in autophagic flux and generally high levels of autophagy-related gene expression relative to other RPE culture models. With each decade past 50 years-old, however, autophagic flux began to plateau and then declined in the most aged RPE cultures, to a nadir at 91 year-old RPE. Feeding 91 year-old RPE POS for a short period did increase autophagic capacity, however it is unsure if that is sustainable over longer feeding periods. It is important to consider that this is a limited sample size, and that there are inherent differences between the adult RPE cultures. Future studies will expand the sample size and include multiple adult RPE cultures of the same age to account for this inherent variability.

Lastly, ARPE-19 was distinct as a RPE culture model that did not fit into a

specific phenotypic age on this spectrum. Although ARPE-19 is a commonly used culture model for RPE studies, an emerging theme throughout this project was ARPE-19's differing characteristics, morphology, and response to autophagy modulators compared to the other RPE culture models. Our results suggest that ARPE-19 is not an appropriate "healthy" model of native RPE, and this should be taken into account for future studies. Accordingly, ARPE-19 is not included in the revised Figure 22.

A limitation of this study was that among the fetal and iPS-RPE, there are also inherent differences in the tissue samples. To ensure reliability of results, the highest quality cell line was used for the iPS-RPE experiments, and data was acquired from at least two biological repeats. Thus, over the course of this one-year project, there were times when I was only able to generate data from a limited sample size. Accordingly, the results from this study may be considered provisional, but will lay the foundation for a more complete study.

In conclusion, this project offered methodology to evaluate phenotypic age in available RPE cell lines, and, further, to induce aging in "immature" RPE models (e.g., hfRPE) via exposure to POS and autophagy manipulation. This project also provided a more thorough comparison of the autophagy- and maturation-related gene expression between the various available RPE cells, allowing quantitative analysis of the differences in expression capabilities between the lines. Additionally, this project offers a novel way to study AMD—specifically, investigating the disease *in vitro* as it develops and presents *in vivo*, i.e., throughout an individual's lifetime, in an aged phenotype. This project has opened an avenue of study to identify target genes that can be manipulated in the autophagy pathway based on differences between phenotypically "young" and "aged"

RPE culture models. Candidate genes will be those that appear to be rate-limiting steps of the autophagic pathway. For future studies, siRNA will be used to knockdown candidate genes in “immature” RPE, and adenoviral vectors will be employed to exogenously express them in “aged” RPE. The ability of pharmaceuticals to regulate these genes and address the impaired pathway will then be tested. Such future studies will move this research into the realm of additional translational research, bringing the bench to the bedside and offering a chance for clinical improvement for those afflicted with AMD.

References:

1. Friedman, D.S., et al., *Prevalence of age-related macular degeneration in the United States.* Arch Ophthalmol, 2004. **122**(4): p. 564-72.

2. Gopinath, B., et al., *Age-related macular degeneration and 5-year incidence of impaired activities of daily living.* Maturitas, 2014. **77**(3): p. 263-6.

3. Young, R.W., *Pathophysiology of age-related macular degeneration.* Survey of Ophthalmology, 1987. **31**(5): p. 291-306.

4. Green, W.R. and C. Enger, *Age-related macular degeneration histopathologic studies. The 1992 Lorenz E. Zimmerman Lecture.* Ophthalmology, 1993. **100**(10): p. 1519-35.

5. Ambati, J. and B.J. Fowler, *Mechanisms of age-related macular degeneration.* Neuron, 2012. **75**(1): p. 26-39.

6. Sobrin, L. and J.M. Seddon, *Nature and nurture- genes and environment- predict onset and progression of macular degeneration.* Progress in Retinal and Eye Research, 2014. **40**(0): p. 1-15.

7. Seddon, J.M., et al., *The US twin study of age-related macular degeneration: relative roles of genetic and environmental influences.* Arch Ophthalmol, 2005. **123**(3): p. 321-7.

8. Haines, J.L., et al., *Complement factor H variant increases the risk of age-related macular degeneration.* Science, 2005. **308**(5720): p. 419-21.

9. Ni Dhubhghaill, S.S., et al., *The pathophysiology of cigarette smoking and age-related macular degeneration.* Adv Exp Med Biol, 2010. **664**: p. 437-46.

10. Ratnapriya, R. and E.Y. Chew, *Age-related macular degeneration – clinical review and genetics update.* Clinical Genetics, 2013. **84**(2): p. 160-166.

11. Young, R.W., *The renewal of photoreceptor cell outer segments.* J Cell Biol, 1967. **33**(1): p. 61-72.

12. Young, R.W. and D. Bok, *Participation of the retinal pigment epithelium in the rod outer segment renewal process.* J Cell Biol, 1969. **42**(2): p. 392-403.

13. Young, R.W. and B. Droz, *The renewal of protein in retinal rods and cones.* J Cell Biol, 1968. **39**(1): p. 169-84.

14. Mazzoni, F., H. Safa, and S.C. Finnemann, *Understanding photoreceptor outer segment phagocytosis: use and utility of RPE cells in culture.* Exp Eye Res, 2014. **126**: p. 51-60.

15. Ruggiero, L. and S. Finnemann, *Rhythmicity of the Retinal Pigment Epithelium*, in *The Retina and Circadian Rhythms*, G. Tosini, et al., Editors. 2014, Springer New York. p. 95-112.

16. McHenry, C.L., et al., *MERTK arginine-844-cysteine in a patient with severe rod-cone dystrophy: loss of mutant protein function in transfected cells.* Invest Ophthalmol Vis Sci, 2004. **45**(5): p. 1456-63.

17. Ostergaard, E., et al., *A novel MERTK deletion is a common founder mutation in the Faroe Islands and is responsible for a high proportion of retinitis pigmentosa cases.* Mol Vis, 2011. **17**: p. 1485-92.

18. Xu, Y.-T., et al., *Age-related maculopathy susceptibility 2 participates in the phagocytosis functions of the retinal pigment epithelium.* International Journal of Ophthalmology, 2012. **5**(2): p. 125-132.

19. Algvere, P.V. and S. Seregard, *Age-related maculopathy: pathogenetic features and new treatment modalities.* Acta Ophthalmologica Scandinavica, 2002. **80**(2): p. 136-143.

20. Arjamaa, O., et al., *Regulatory role of HIF-1alpha in the pathogenesis of age-related macular degeneration (AMD).* Ageing Res Rev, 2009. **8**(4): p. 349-58.

21. Terman, A. and U.T. Brunk, *Lipofuscin.* Int J Biochem Cell Biol, 2004. **36**(8): p. 1400-4.

22. Krohne, T.U., F.G. Holz, and J. Kopitz, *Apical-to-basolateral transcytosis of photoreceptor outer segments induced by lipid peroxidation products in human retinal pigment epithelial cells.* Invest Ophthalmol Vis Sci, 2010. **51**(1): p. 553-60.

23. Kaarniranta, K., *Autophagy – hot topic in AMD.* Acta Ophthalmologica, 2010. **88**(4): p. 387-388.

24. Kaarniranta, K., et al., *Heat shock proteins as gatekeepers of proteolytic pathways-Implications for age-related macular degeneration (AMD).* Ageing Res Rev, 2009. **8**(2): p. 128-39.

25. Levine, B. and D.J. Klionsky, *Development by self-digestion: molecular mechanisms and biological functions of autophagy.* Dev Cell, 2004. **6**(4): p. 463-77.

26. Tsukada, M. and Y. Ohsumi, *Isolation and characterization of autophagy-defective mutants of Saccharomyces cerevisiae.* FEBS Lett, 1993. **333**(1-2): p. 169-74.

27. Klionsky, D.J., et al., *A unified nomenclature for yeast autophagy-related genes.* Dev Cell, 2003. **5**(4): p. 539-45.

28. Kihara, A., et al., *Beclin-phosphatidylinositol 3-kinase complex functions at the trans-Golgi network.* EMBO Rep, 2001. **2**(4): p. 330-5.

29. Codogno, P., M. Mehrpour, and T. Proikas-Cezanne, *Canonical and non-canonical autophagy: variations on a common theme of self-eating?* Nat Rev Mol Cell Biol, 2012. **13**(1): p. 7-12.

30. Liu, J., et al., *Beclin1 Controls the Levels of p53 by Regulating the Deubiquitination Activity of USP10 and USP13.* Cell, 2011. **147**(1): p. 223-234.

31. Weber, J.D. and D.H. Gutmann, *Deconvoluting mTOR biology.* Cell Cycle, 2012. **11**(2): p. 236-48.

32. Tanemura, M., et al., *Rapamycin causes upregulation of autophagy and impairs islets function both in vitro and in vivo.* Am J Transplant, 2012. **12**(1): p. 102-14.

33. Spilman, P., et al., *Inhibition of mTOR by rapamycin abolishes cognitive deficits and reduces amyloid-beta levels in a mouse model of Alzheimer's disease.* PLoS One, 2010. **5**(4): p. e9979.

34. Malagelada, C., et al., *Rapamycin protects against neuron death in in vitro and in vivo models of Parkinson's disease.* J Neurosci, 2010. **30**(3): p. 1166-75.

35. Zhu, J.H., et al., *Regulation of autophagy by extracellular signal-regulated protein kinases during 1-methyl-4-phenylpyridinium-induced cell death.* Am J Pathol, 2007. **170**(1): p. 75-86.

36. Arsov, I., et al., *A role for autophagic protein beclin 1 early in lymphocyte development.* J Immunol, 2011. **186**(4): p. 2201-9.

37. Mestre, M.B., et al., *Alpha-hemolysin is required for the activation of the autophagic pathway in Staphylococcus aureus-infected cells.* Autophagy, 2010. **6**(1): p. 110-25.

38. Grishchuk, Y., et al., *Beclin 1-independent autophagy contributes to apoptosis in cortical neurons.* Autophagy, 2011. **7**(10): p. 1115-31.

39. Sarkar, S., et al., *Lithium induces autophagy by inhibiting inositol monophosphatase.* J Cell Biol, 2005. **170**(7): p. 1101-11.

40. Salminen, A. and K. Kaarniranta, *Regulation of the aging process by autophagy.* Trends Mol Med, 2009. **15**(5): p. 217-24.

41. Ryhanen, T., et al., *Crosstalk between Hsp70 molecular chaperone, lysosomes and proteasomes in autophagy-mediated proteolysis in human retinal pigment epithelial cells.* J Cell Mol Med, 2009. **13**(9b): p. 3616-31.

42. Wang, A.L., et al., *Autophagy and exosomes in the aged retinal pigment epithelium: possible relevance to drusen formation and age-related macular degeneration.* PLoS One, 2009. **4**(1): p. e4160.

43. Vittal Rao H, C.J., Afzal A, Grant MB, Akin D, Dunn WA, Kim JS, Hageman GS, Boulton ME, *A decline in autophagic efficiency is associated with AMD and chronic exposure to oxidative stress.* Invest Ophthalmol Vis Sci, 2009. **50**: p. ARVO E-Abstract 4182.

44. Cemma, M. and J.H. Brumell, *Interactions of pathogenic bacteria with autophagy systems.* Curr Biol, 2012. **22**(13): p. R540-5.

45. Rizzolo, L.J., et al., *Integration of tight junctions and claudins with the barrier functions of the retinal pigment epithelium.* Progress in Retinal and Eye Research, 2011. **30**(5): p. 296-323.

46. Peng, S., et al., *Effects of proinflammatory cytokines on the claudin-19 rich tight junctions of human retinal pigment epithelium.* Invest Ophthalmol Vis Sci, 2012. **53**(8): p. 5016-28.

47. Peng, S., et al., *Engineering a blood-retinal barrier with human embryonic stem cell-derived retinal pigment epithelium: transcriptome and functional analysis.* Stem Cells Transl Med, 2013. **2**(7): p. 534-44.

48. Schwartz, S.D., et al., *Human embryonic stem cell-derived retinal pigment epithelium in patients with age-related macular degeneration and Stargardt's macular dystrophy: follow-up of two open-label phase 1/2 studies.* Lancet, 2014.

49. Takahashi, K. and S. Yamanaka, *Induction of pluripotent stem cells from mouse embryonic and adult fibroblast cultures by defined factors.* Cell, 2006. **126**(4): p. 663-76.

50. Takahashi, K., et al., *Induction of pluripotent stem cells from adult human fibroblasts by defined factors.* Cell, 2007. **131**(5): p. 861-72.

51. Yu, J., et al., *Induced pluripotent stem cell lines derived from human somatic cells.* Science, 2007. **318**(5858): p. 1917-20.

52. Buchholz, D.E., et al., *Derivation of functional retinal pigmented epithelium from induced pluripotent stem cells.* Stem Cells, 2009. **27**(10): p. 2427-34.

53. Carr, A.-J., et al., *Protective Effects of Human iPS-Derived Retinal Pigment Epithelium Cell Transplantation in the Retinal Dystrophic Rat.* PLoS ONE, 2009. **4**(12): p. e8152.

54. Phillips, M.J., et al., *Blood-derived human iPS cells generate optic vesicle-like structures with the capacity to form retinal laminae and develop synapses.* Invest Ophthalmol Vis Sci, 2012. **53**(4): p. 2007-19.

55. Salero, E., et al., *Adult Human RPE Can Be Activated into a Multipotent Stem Cell that Produces Mesenchymal Derivatives.* Cell Stem Cell, 2012. **10**(1): p. 88-95.

56. Wright, L.S., et al., *Induced pluripotent stem cells as custom therapeutics for retinal repair: Progress and rationale.* Experimental Eye Research, 2014. **123**(0): p. 161-172.

57. Kokkinaki, M., N. Sahibzada, and N. Golestaneh, *Human induced pluripotent stem-derived retinal pigment epithelium (RPE) cells exhibit ion transport, membrane potential, polarized vascular endothelial growth factor secretion, and gene expression pattern similar to native RPE.* Stem Cells, 2011. **29**(5): p. 825-35.

58. Stern, J. and S. Temple, *Stem cells for retinal repair.* Dev Ophthalmol, 2014. **53**: p. 70-80.

59. Schutt, F., et al., *Moderately reduced ATP levels promote oxidative stress and debilitate autophagic and phagocytic capacities in human RPE cells.* Invest Ophthalmol Vis Sci, 2012. **53**(9): p. 5354-61.

60. Wang, A.L., et al., *Using LC3 to Monitor Autophagy Flux in the Retinal Pigment Epithelium.* Autophagy, 2009. **5**(8): p. 1190-1193.

61. Blenkinsop, T.A., et al., *The culture and maintenance of functional retinal pigment epithelial monolayers from adult human eye.* Methods Mol Biol, 2013. **945**: p. 45-65.

62. Dunn, K.C., et al., *ARPE-19, a human retinal pigment epithelial cell line with differentiated properties.* Exp Eye Res, 1996. **62**(2): p. 155-69.

63. Ahmado, A., et al., *Induction of differentiation by pyruvate and DMEM in the human retinal pigment epithelium cell line ARPE-19.* Invest Ophthalmol Vis Sci, 2011. **52**(10): p. 7148-59.

64. Luo, Y., et al., *Effects of culture conditions on heterogeneity and the apical junctional complex of the ARPE-19 cell line.* Invest Ophthalmol Vis Sci, 2006. **47**(8): p. 3644-55.

65. Westenskow, P.D., et al., *Using Flow Cytometry to Compare the Dynamics of Photoreceptor Outer Segment Phagocytosis in iPS-Derived RPE Cells.* Investigative Ophthalmology & Visual Science, 2012. **53**(10): p. 6282-6290.

66. Ablonczy, Z., et al., *Human Retinal Pigment Epithelium Cells as Functional Models for the RPE In Vivo.* Investigative Ophthalmology & Visual Science, 2011. **52**(12): p. 8614-8620.

67. Peng, S., et al., *Claudin-19 and the barrier properties of the human retinal pigment epithelium.* Invest Ophthalmol Vis Sci, 2011. **52**(3): p. 1392-403.

68. Idelson, M., et al., *Directed differentiation of human embryonic stem cells into functional retinal pigment epithelium cells.* Cell Stem Cell, 2009. **5**(4): p. 396-408.

69. Ferrer, M., et al., *A multiplex high-throughput gene expression assay to simultaneously detect disease and functional markers in induced pluripotent stem cell-derived retinal pigment epithelium.* Stem Cells Transl Med, 2014. **3**(8): p. 911-22.

70. Carvajal-Vergara, X., et al., *Patient-specific induced pluripotent stem-cell-derived models of LEOPARD syndrome.* Nature, 2010. **465**(7299): p. 808-12.

71. Maminishkis, A., et al., *Confluent monolayers of cultured human fetal retinal pigment epithelium exhibit morphology and physiology of native tissue.* Invest Ophthalmol Vis Sci, 2006. **47**(8): p. 3612-24.

72. Livak, K.J. and T.D. Schmittgen, *Analysis of relative gene expression data using real-time quantitative PCR and the 2(-Delta Delta C(T)) Method.* Methods, 2001. **25**(4): p. 402-8.

73. Klionsky, D.J., et al., *Guidelines for the use and interpretation of assays for monitoring autophagy.* Autophagy, 2012. **8**(4): p. 445-544.

74. Peng, S., R.A. Adelman, and L.J. Rizzolo, *Minimal effects of VEGF and anti-VEGF drugs on the permeability or selectivity of RPE tight junctions.* Invest Ophthalmol Vis Sci, 2010. **51**(6): p. 3216-25.

75. Mao, Y. and S.C. Finnemann, *Analysis of Photoreceptor Outer Segment Phagocytosis by RPE Cells in Culture.* Methods in molecular biology (Clifton, N.J.), 2013. **935**: p. 285-295.

76. Petrou, P.A., et al., *Intravitreal Sirolimus for the Treatment of Geographic Atrophy: Results of a Phase I/II Clinical Trial.* Invest Ophthalmol Vis Sci, 2015. **56**(1): p. 330-8.

77. Wong, W.T., et al., *Treatment of Geographic Atrophy With Subconjunctival Sirolimus: Results of a Phase I/II Clinical Trial.* Investigative Ophthalmology & Visual Science, 2013. **54**(4): p. 2941-2950.

78. Kim, J.Y., et al., *Noncanonical autophagy promotes the visual cycle.* Cell, 2013. **154**(2): p. 365-76.

79. Wang, H.C., et al., *Profiling the microRNA Expression in Human iPS and iPS-derived Retinal Pigment Epithelium.* Cancer Inform, 2014. **13**(Suppl 5): p. 25-35.

80. Kamao, H., et al., *Characterization of Human Induced Pluripotent Stem Cell-Derived Retinal Pigment Epithelium Cell Sheets Aiming for Clinical Application.* Stem Cell Reports, 2014. **2**(2): p. 205-218.